Available online at www.sciencedirect.com
ScienceDirect
Planetary and Space Science 56 (2008) 985–1013
Planetary and Space Science
www.elsevier.com/locate/pss

Recent geological and hydrological activity on Mars: The Tharsis/Elysium corridor

James M. Dohm[a,b,*], Robert C. Anderson[c], Nadine G. Barlow[d], Hirdy Miyamoto[e], Ashley G. Davies[c], G. Jeffrey Taylor[f], Victor R. Baker[a,b], William V. Boynton[b], John Keller[b], Kris Kerry[b], Daniel Janes[b], Alberto G. Fairén[g,h], Dirk Schulze-Makuch[i], Mihaela Glamoclija[j], Lucia Marinangeli[j], Gian G. Ori[j], Robert G. Strom[b], Jean-Pierre Williams[k], Justin C. Ferris[l], J.A.P. Rodríguez[m], Miguel A. de Pablo[n], Suniti Karunatillake[o]

[a]*Department of Hydrology and Water Resources, University of Arizona, Tucson, AZ 85721, USA*
[b]*Lunar and Planetary Laboratory, University of Arizona, Tucson, AZ 85721, USA*
[c]*Jet Propulsion Laboratory, California Institute of Techonolgy, Pasadena, CA 91109, USA*
[d]*Department of Physics and Astronomy, Northern Arizona University, Flagstaff, AZ 86011, USA*
[e]*Department of Geosystem Engineering, University of Tokyo, Japan*
[f]*Hawai'i Institute of Geophysics and Planetology, University of Hawai'i, Honolulu, Hawai'i 96822, USA*
[g]*Centro de Biología Molecular, CSIC-Universidad Autónoma de Madrid, 28049 Cantoblanco, Madrid, Spain*
[h]*Space Science and Astrobiology, Division, NASA Ames Research Center, Moffett Field, CA 94035, USA*
[i]*School of Earth and Environmental Sciences, Washington State University, Pullman, WA 99164, USA*
[j]*IRSPS, Università d'Annunzio, Pescara, Italy*
[k]*Division of Geological and Planetary Sciences, California Institute of Technology, Pasadena, CA 91125, USA*
[l]*West Coast and Alaska Tsunami Warning Center, National Oceanic and Atmospheric Administration, Palmer, AK 99645, USA*
[m]*Department of Earth and Planetary Science, University of Tokyo, 7-3-1 Hongo, Bunkyo-ku, Tokyo 113-0033, Japan*
[n]*Departamento de Geología, Universidad de Alcalá, 28871 Alcalá de Henares, Madrid, Spain*
[o]*Center for Radiophysics and Space Research, Cornell University, Ithaca, NY 14853, USA*

Received 8 November 2006; received in revised form 24 November 2007; accepted 1 January 2008
Available online 17 January 2008

Abstract

The paradigm of an ancient warm, wet, and dynamically active Mars, which transitioned into a cold, dry, and internally dead planet, has persisted up until recently despite published Viking-based geologic maps that indicate geologic and hydrologic activity extending into the Late Amazonian epoch. This paradigm is shifting to a water-enriched planet, which may still exhibit internal activity, based on a collection of geologic, hydrologic, topographic, chemical, and elemental evidences obtained by the Viking, Mars Global Surveyor (MGS), Mars Odyssey (MO), Mars Exploration Rovers (MER), and Mars Express (MEx) missions. The evidence includes: (1) stratigraphically young rock materials such as pristine lava flows with few, if any, superposed impact craters; (2) tectonic features that cut stratigraphically young materials; (3) features with possible aqueous origin such as structurally controlled channels that dissect stratigraphically young materials and anastomosing-patterned slope streaks on hillslopes; (4) spatially varying elemental abundances for such elements as hydrogen (H) and chlorine (Cl) recorded in rock materials up to 0.33 m depth; and (5) regions of elevated atmospheric methane. This evidence is pronounced in parts of Tharsis, Elysium, and the region that straddles the two volcanic provinces, collectively referred to here as the Tharsis/Elysium corridor. Based in part on field investigations of Solfatara Crater, Italy, recommended as a suitable terrestrial analog, the Tharsis/Elysium corridor should be considered a prime target for Mars Reconnaissance Orbiter (MRO)

*Corresponding author. Department of Hydrology and Water Resources, University of Arizona, Tucson, AZ 85721, USA. Tel.: +1 520 626 8454; fax: +1 520 6211422.
E-mail address: jmd@hwr.arizona.edu (J.M. Dohm).

0032-0633/$ - see front matter
doi:10.1016/j.pss.2008.01.001

investigations and future science-driven exploration to investigate whether Mars is internally and hydrologically active at the present time, and whether the persistence of this activity has resulted in biologic activity.

Keywords: Mars; Magmatism; Tectonism; Hydrothermal activity; Present Mars; Life

1. Introduction

The small size of Mars (~53% of Earth's diameter) and other geophysical constraints have led to the theory that Mars experienced an early rapid loss of internal heat energy with subsequent steady-state decline (Spohn, 1991; Schubert et al., 1992; McGovern et al., 2002). This contributed to the Viking-era paradigm of an ancient warm, wet, and dynamically active planet, which transitioned into a cold, dry, and internally dead world (e.g., Pollack et al., 1987; Carr, 1996). This paradigm persisted in spite of being contradicted by Viking-based geologic mapping on global to local scales that indicated a water-enriched, geologically and hydrologically active planet as recent as the Late Amazonian epoch (e.g., Scott and Tanaka, 1986; Greeley and Guest, 1987); equivalent to an estimated absolute age of ~300 million years, based on the Mars cratering chronology of Hartmann and Neukum (2001). New Mars Global Surveyor (MGS)-, Mars Odyssey (MO)-, and Mars Express (MEx)-based information collectively point to a planet which has been geologically active up to the present day, particularly in parts of the Tharsis and Elysium volcanic provinces and the region that straddles both volcanic provinces. Throughout the rest of this paper, we will refer to this region as the Tharsis/Elysium corridor (Fig. 1).

The corridor was first identified as a region of protracted geologic and hydrologic activity from stratigraphic, paleotectonic, topographic, impact crater, hydrologic, geomorphic, and geophysical information obtained through Viking and MGS analyses (Figs. 1 and 2). We have extended our initial studies by incorporating data from MO and MEx, particularly MO's Thermal Emission Imaging System (THEMIS) visible (VIS) and daytime infrared (IR) imagery and the newly released elemental data (especially H and Cl) from GRS. The presented work is a synthesis of both old and new information that reveals a diverse and far-reaching (Table 1) geologic history with important implications for the geodynamic evolution of Mars.

We have compiled many unique characteristics of the Tharsis/Elysium corridor. Each can be interpreted in several different ways, but a single consistent history is revealed when one considers the entirety of geologic and composition data which are now available. In this paper,

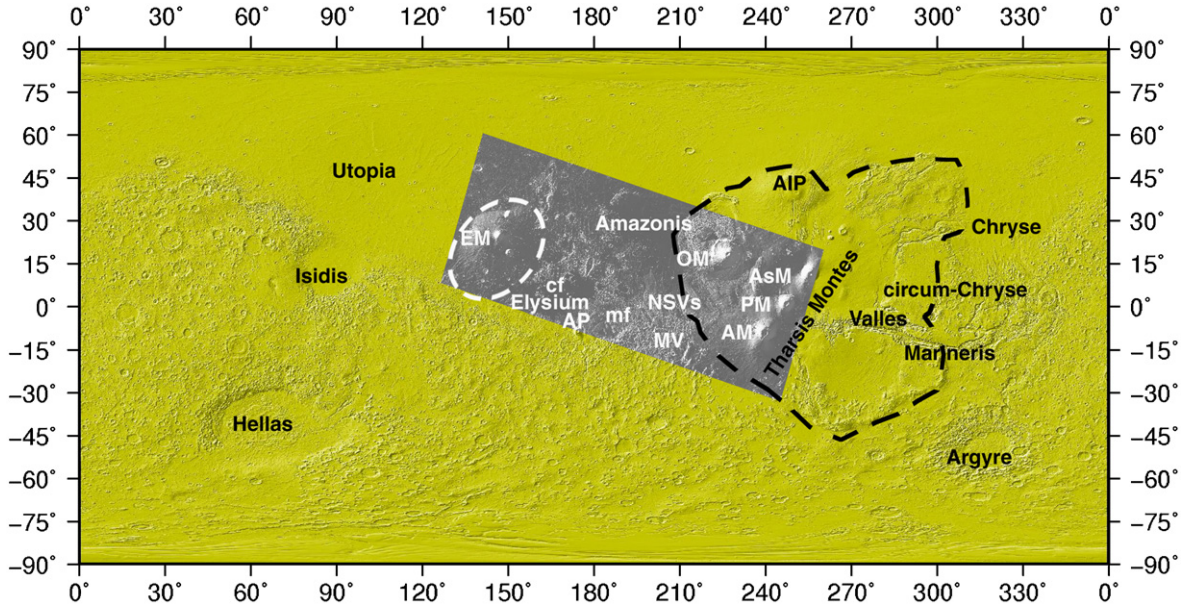

Fig. 1. MOLA map highlighting (gray tone) Tharsis/Elysium corridor region, which includes parts of Tharsis and Elysium volcanic provinces (dashed line shows their approximate boundaries), and the region that straddles their boundaries. Features discussed in the text include the Tharsis Montes shield volcanoes, Arsia Mons (AM), Pavonis Mons (PM), Ascraeus Mons (AsM), Olympus Mons (OM), Northwestern Slope Valleys (NSVs), Mangala Valles (MV), Amazonis and Elysium basins, Cerebus Fossae (cf), Alba and Apollinaris Paterae (AlP and AP, respectively), Elysium Mons (EM), and general location of Medusae Fossae Formation materials (mf). Importantly, the boundary is only roughly defined and schematically shown here. The boundary will be mapped more accurately in the future through continued exploration to Mars. For example, Alba Patera (AlP) and other parts of Tharsis might be added to the corridor region, as possibly indicated by the pit crater chains that mark the martian surface near the southeast margin of the shield volcano (also see Wyrick et al., 2004).

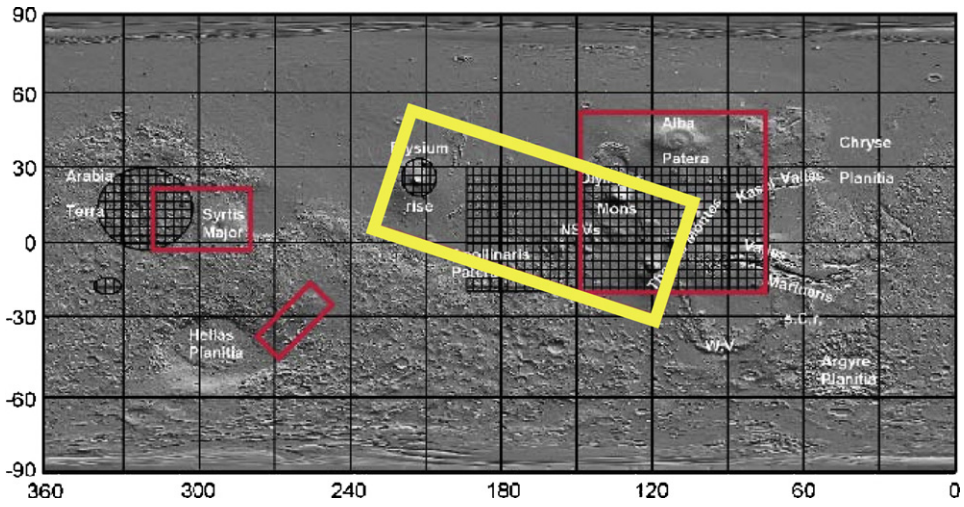

Fig. 2. MOLA shaded relief image showing general locations of anomalous concentrations of dark slope streaks indicated by hachured patterns (adapted from Rifkin and Mustard, 2001). In addition to the proposal of dust avalanching (Sullivan et al., 2001), water may have also contributed to their formation (Schorghofer et al., 2002), especially since they occur in regions that record long-lived magmatic and hydrologic activity (Ferris et al., 2002) and several display anastomosing patterns. Potential regions of elevated heat flow initially identified for THEMIS investigation (red boxes) based on stratigraphic, tectonic, paleohydrologic, geomorphologic, impact crater, and geophysical information. Subsequent evaluation of the GRS-based Cl information mapped to the previously identified Corridor region (yellow box).

we present evidence that the Tharsis/Elysium corridor is a region that records diverse and far-reaching magmatic, tectonic, and fluvial activity, continuing at least until geologically recent time, well into the Late Amazonian (Table 1). The evidence includes:

- Pristine lava flows of Tharsis Montes with few if any superposed impact craters (Hartmann et al., 1999; Neukum et al., 2004).
- Structurally controlled releases of water and other possible volatiles from Cerberus Fossae (e.g., Burr et al., 2002; Mitchell and Wilson, 2003), as well as structurally controlled channels that dissect Amazonian lavas of Tharsis Montes and Medusae Fossae Formation materials (Mouginis-Mark, 1990; Scott et al., 1993, 1995; Dohm et al., 2004).
- The occurrence of anastomosing dark slope streaks in Mangala Valles and the northwestern slope valleys (NSVs) regions, which may be indicative of aqueous activity (Ferris et al., 2002; Miyamoto et al., 2004). These regions have recorded magmatic, tectonic, and hydrologic activity since the Noachian Period (Dohm et al., 2001a, b, 2004).
- Tectonic features such as fractures, faults, graben, and structurally controlled pit crater chains that cut stratigraphically young rock materials, including the flanks and aureole deposits of the Tharsis Montes shield volcanoes, plains-forming materials in the corridor region, and Elysium rise-forming materials (Scott and Zimbelman, 1995; Scott et al., 1998; Anderson et al., 2001; Wyrick et al., 2004; Ferrill et al., 2004; Márquez et al., 2004).
- Geologic terrains that display few if any superposed impact craters (Hartmann et al., 1999; Neukum et al., 2004), such as the Ceberus Fossae region where impact crater counts of the adjacent fluvially dissected plains range from 10 to 100 Myr (Burr et al., 2002; Berman and Hartmann, 2002).
- MO Gamma Ray Spectrometer (GRS)-based elevated hydrogen (H) and chlorine (Cl) recorded in rock materials up to 0.33 m depth in the NSVs region and other regions along the highland-lowland boundary west of the Tharsis Montes shield volcanoes (Boynton et al., 2002, 2007, in press; Feldman et al., 2002; Keller et al., 2006). This broad region records magmatic, tectonic, and hydrologic activity extending from the Noachian to the Late Amazonian (Scott and Tanaka, 1986; Greeley and Guest, 1987), indicating possible hydrothermal environments for parts of the region (Dohm et al., 2004; Schulze-Makuch et al., 2007).
- Regions with elevated elemental abundances of methane (CH_4), detected by the Planetary Fourier Spectrometer instrument on MEx (Formisano et al., 2004) and Earth-based observations (Mumma et al., 2004; Krasnopolshy et al., 2004). Magmatism, hydrothermal activity, and biological release are a few of the possible explanations for the CH_4 (Formisano et al., 2004; Prieto-Ballesteros et al., 2006; Krasnopolsky, 2006; Onstott et al., 2006).

Most thermal models suggest that Mars reached a stagnant-lid regime early in its history, leading to lithospheric conduction as the primary mechanism for removal of internal heat (Sleep, 2000; Breuer and Spohn, 2003). In addition to lithospheric conduction, plumes during the stagnant-lid regime, ranging from superplumes (Dohm et al., 2001a, 2002b, 2007a, b; Baker et al., 2007) to mantle plumes (Mège and Ernst, 2001), have produced regional to local enhanced magmatic and tectonic activity.

Table 1
Geology, tectonism, hydrology, and geochemical activity of the Tharsis, Elysium, and Tharsis/Elysium corridor regions through time (Early Noachian—EN, Middle Noachian—MN, Late Noachian—LN, Early Hesperian—EH, Late Hesperian—LH, Early Amazonian—EA, Middle Amazonian—MA, Late Amazonian—LA). Note that the commencement and/or end of activity of the all listed features are not absolutely constrained and only those features in the corridor region shown in bold

Activity (mountain building, tectonism, magmatic-driven activity, which may include uplift, tectonism, volcanism, and possibly hydrothermal activity, water-related activity, and geochemical formation)	**EN**	**MN**	**LN**	**EH**	**LH**	**EA**	**MA**	**LA**
Pre-Tharsis development of the Thaumasia highlands mountain range (Dohm et al., 2001a, c); *possible reactivation of ancient basement structures into the Hesperian related the evolution of Tharsis, which includes the development of a thrust belt (Schultz and Tanaka, 1994) and rift systems (Dohm et al., 2001c; Grott et al., 2007)	→	→*						
Pre-Tharsis development of the Coprates rise mountain range (Schultz and Tanaka, 1994; Dohm et al., 2001a, c); *possible reactivation of ancient basement structures into the Hesperian related the evolution of Tharsis, which includes the development of a thrust belt (Schultz and Tanaka, 1994)	→	→*						
Widespread Tectonism (Scott and Dohm, 1997; Anderson et al., 2001, 2007a; Dohm et al., 2001c)	→	→	→					
Magmatic-tectonic activity at Claritas rise, possibly pre-Tharsis (Anderson et al., 2001; Dohm et al., 2001a, c)	→	→						
Widespread valley formation and relatively high erosion rate (Pieri, 1976; Scott et al., 1995; Carr and Chuang, 1997; Baker et al., 2007)	→	→	→					
Clays (e.g., Bibring et al., 2006)	→	→						
Tharsis development, which includes five major stages of activity (e.g., Dohm et al., 2001, 2007a; Baker et al., 2007)		→	→	→	→	→	→	→
Tharsis basin, including diminishing water supply through time (Dohm et al., 2001a)		→	→					
Sulfates (e.g., Bibring et al., 2006)			→	→	→			
Magmatic-tectonic activity in the Ceraunius rise region (Anderson et al., 2001, 2004)		→	→					
Development of Tempe Terra igneous plateau, which includes magmatic–tectonic activity and volcanism (Scott and Tanaka, 1986; Scott and Dohm, 1990a, b; Anderson et al., 2001; Moore, 2001)		→	→	→	→	→		
Magmatic–tectonic activity in the Uranius Patera region (Anderson et al., 2001)		→	→					
Thaumasia plateau uplift (Dohm and Tanaka, 1999; Dohm et al., 2001c)		→	→	→				
Putative ocean that covered ~1/3 of the surface area of Mars, possibly associated with the incipient development of the Tharsis superplume (Parker et al., 1993; Clifford and Parker, 2001; Fairén et al., 2003; Baker et al., 2007; Dohm et al., 2007a), which includes endogenic-driven acidic conditions (Fairén et al., 2004)		→	→					
Emplacement of older ridged plains materials in the Thaumasia Planum region (Dohm and Tanaka, 1999; Dohm et al., 2001c)			→	→				
Patera-forming at Apollinaris (Scott et al., 1993; Robinson et al., 1993)			→	→				
Patera-forming at Tempe (Scott and Tanaka, 1986; Scott and Dohm, 1990a, b)			→	→				
Construction of isolated volcanoes in the Thaumasia highlands and Coprates rise region (Dohm et al., 2001c)			→	→				
Magmatic–tectonic activity, which includes uplift at the central part of Valles Marineris (Dohm et al., 1998, 2001a, b, 2007a; Anderson et al, 2001)			→	→				

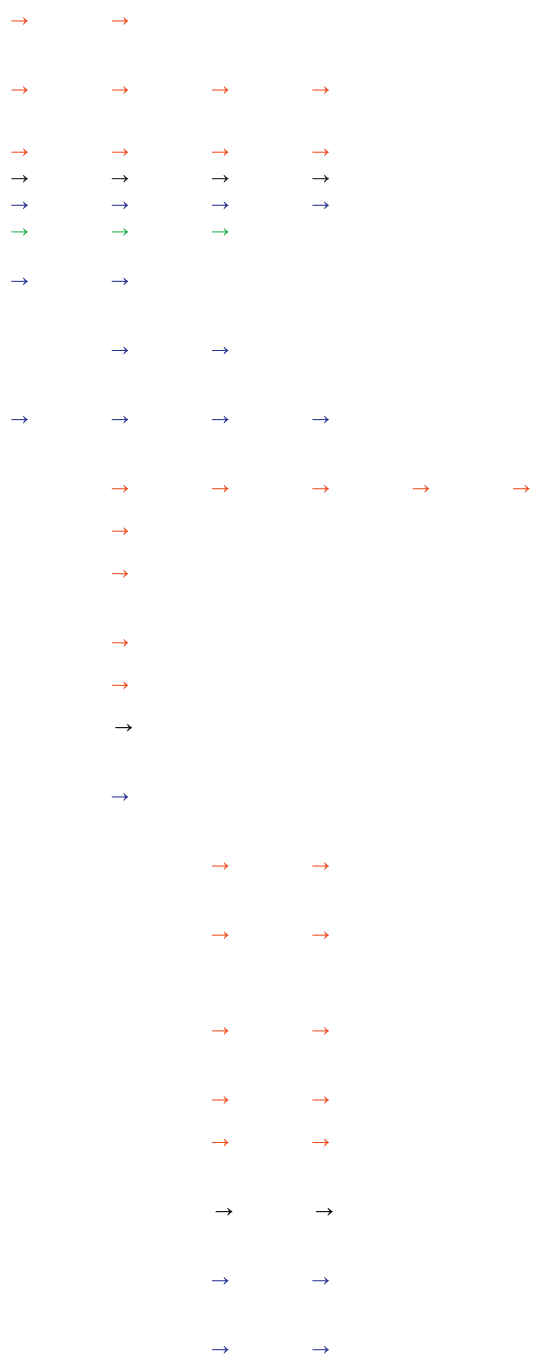

Magmatic-tectonic activity, which includes uplift at Warrego rise (Gulick, 1998; Dohm et al., 1998, 2001a, c; Anderson et al., 2001)

Development of Syria Planum, a corona-like feature (Wise et al., 1979; Plescia and Saunders, 1982; Tanaka and Davis, 1988; Golombek, 1989; Dohm et al., 1998, 2001a, c; Anderson et al., 2001, 2004)

Valles Marineris development, which includes magmatic-driven uplift and tectonism, volcanism, sapping, collapse, outflow channel activity, and formation of sulfate deposits (Lucchitta et al., 1992; Banerdt et al., 1992; Tanaka et al., 1991; Dohm and Tanaka, 1999, 2001a–c, 2007a, b; Komatsu et al., 2004; Bibring et al., 2006)

Early circum-Chryse and **northwestern slope valleys (NSVs) outflow channel development (Rotto and Tanaka, 1995; Nelson and Greeley, 1999; Dohm et al., 2001a, b)**

Valley network development not as widespread when compared to the Noachian Period (Gulick, 1993; Scott et al., 1995; Carr and Chuang, 1997; Tanaka et al., 1998; Dohm and Tanaka, 1999; Dohm et al., 2001c)

Episodic outflow channel development of Ma'adim Valles (Greeley and Guest, 1987; Scott et al., 1993; Cabrol et al., 1998; Kuzmin et al., 2004), though a single catastrophic flood event has also been reported (Irwin et al., 2002)

Elysium rise development (Greeley and Guest, 1987; Tanaka et al., 1992; Tanaka et al., 2005)

Emplacement of younger ridged plains (unit Hr; Scott and Tanaka, 1986; Greeley and Guest, 1987)

Magmatic-tectonic activity in a region northeast of Pavonis (pre-Tharsis Montes; Plescia et al., 1980; Anderson et al., 2001)

Magmatic-tectonic activity in the southwest part of Tempe Terra (Anderson et al., 2001)

Magmatic–tectonic activity in the Ulysses Fossae region (pre-Tharsis Montes?; Anderson et al., 2001)

Widespread but less tectonism when compared to the Noachian Period (Scott and Dohm, 1997; Dohm and Tanaka, 1999; Dohm et al., 2001a, c; Anderson et al., 2001)

Early development of Mangala Valles (Chapman and Tanaka, 1993; Zimbelman et al., 1994; Craddock and Greeley, 1994)

Incipient Tharsis Montes and Olympus Mons development (Scott and Tanaka, 1986; Scott and Zimbelman, 1995; Scott et al., 1995, 1998; Anderson et al., 2001)

Emplacement of lavas centered at Tharsis Montes (Scott and Tanaka, 1986; Scott et al., 1995, 1998), Alba Patera (Scott and Tanaka, 1986), and Syria Planum (Scott and Tanaka, 1986; Dohm and Tanaka, 1999; Dohm et al., 2001c)

Emplacement of lavas centered at Elysium rise (Greeley and Guest, 1987; Tanaka et al., 1992, 2005) and on the southern flank of Apollinaris Patera (Scott et al., 1993; Robinson et al., 1993)

Magmatic-tectonic activity at Alba Patera (Anderson et al., 2001)

Change from widespread Tharsis magmatic-tectonic activity to centralized volcanism to forge the giant shield volcanoes of Tharsis Montes, Olympus Mons, and Alba Patera (Dohm et al., 1999, 2001c)

Significant waning of tectonism in the western hemisphere except at Alba Patera (Scott and Tanaka, 1986; Dohm and Tanaka, 1999, 2001c; Anderson et al, 2001)

Significant outflow channel development, which includes Mangala Valles (Chapman and Tanaka, 1993; Zimbelman et al., 1994; Craddock and Greeley, 1994)

Table 1 (*continued*)

Activity (mountain building, tectonism, magmatic-driven activity, which may include uplift, tectonism, volcanism, and possibly hydrothermal activity, water-related activity, and geochemical formation)	**EN**	**MN**	**LN**	**EH**	**LH**	**EA**	**MA**	**LA**
Significant outflow channel development of the circum-Chryse outflow channel system (Scott and Tanaka, 1986; Chapman et al., 1991; DeHon, 1992; Scott, 1993; Rotto and Tanaka, 1995; Rice and DeHon, 1996; Chapman and Tanaka, 1996; Nelson and Greeley, 1999; Tanaka et al., 2005)								
Putative ocean (Jöns, 1986; Lucchitta et al., 1986; Parker et al., 1987, 1993; McGill, 1985; Baker et al., 1991; Kargel et al., 1995; Head et al., 1999; Clifford and Parker, 2001; Baker et al., 2007; Dohm et al., 2007a) and/or paleolakes (Scott et al., 1995), possibly related to Tharsis and to a lesser extent, Elysium rise activity (Fairén et al., 2003)					→	→?		
Anhydrous ferric oxides (Bibring et al., 2006)					→	→	→	→
Continued construction of Olympus Mons (Scott and Tanaka, 1986; Morris et al., 1991; Morris and Tanaka, 1994; Neukum et al., 2004)					→	→	→	→
Late-stage volcanic activity at Elysium rise (Greeley and Guest, 1987; Tanaka et al., 1992; DeHon et al., 1999; Tanaka et al., 2005)					→	→	→	→
Late-stage volcanic activity at Tharsis Montes, which includes emplacement of the aureole deposits (Scott and Tanaka, 1986; Scott et al., 1995; Scott et al., 1998)					→	→	→	→
Emplacement of the Medusae Fossae materials (Malin, 1979; Scott and Tanaka, 1986; Greeley and Guest, 1987; Tanaka et al., 2005); *though denoted in red, materials could be ash-flow tuffs (Malin, 1979; Scott and Tanaka, 1982, 1986), ancient polar deposits (Schultz and Lutz, 1988), or pyroclastic and eolian materials (Greeley and Guest, 1987)						*→	*→	*→
Magmatic–tectonic activity in a region south of Ascraeus (Anderson et al., 2001)						→	→	→
Local tectonism associated with some of the large shield volcanoes including Tharsis Montes (Scott and Dohm, 1997; Anderson et al., 2001)						→	→	→
Valley formation on the northwest flank of Elysium rise (Tanaka et al., 1992; Scott et al., 1995; DeHon et al., 1999)						→	→	→
Valley formation between Utopia Planitia and the eastern part of Elysium Planitia (Marte Vallis interpreted to be a spillway; Scott et al., 1995)						→	→	→
Valley formation on the northern flank of Alba Patera (Scott et al., 1995; Gulick, 1998)						→	→	→
Valley formation in parts of the northern plains (Scott et al., 1995)						→	→	→
Emplacement of the aureole deposits, interpreted to be the result of late-stage glaciation and interaction between ice and lavas (Scott et al., 1995; Scott and Zimbelman, 1995; Shean et al., 2005)							→	→

The evidence presented in this paper point to the Tharsis/Elysium corridor as a primary region where the internal heat of the planet may be focused through magmatism, tectonism, and hydrologic/hydrogeologic activity. In the following sections, we compile evidence that points to a geologically, hydrogeologically, and possibly a biologically active Tharsis/Elysium corridor region. We argue that the Solfatara volcanic complex in Italy may be an appropriate terrestrial analog to the Tharsis–Elysium corridor. We also present an explanation for why the corridor region may not be thermally distinct in THEMIS observations and why it should be considered a prime target for Mars Express, MRO, and future science-driven exploration. An internally active Mars has tremendous implications for present and future subsurface heat flow and hydrogeology, as well as the potential for extant life.

2. Geologic evidence for an internally active Mars

To address the query of whether Mars is internally active, we have conducted a comparative analysis of the geological, paleohydrological, topographic, geophysical, spectral, and elemental information for Mars. Viking-, MGS-, MO-, and MEx-based information collectively suggest that the Tharsis/Elysium corridor reflects far-reaching, episodic internal activity, and that such activity may continue well into the future.

2.1. Geologic and physiographic setting of the Tharsis/Elysium corridor

The Tharsis/Elysium corridor (Fig. 1) includes parts of the Tharsis (Scott and Tanaka, 1986) and Elysium (Greeley and Guest, 1987) magmatic complexes and the region that straddles the two complexes. The corridor also includes the NSVs region located on the western margin of Tharsis (Dohm et al., 2004), a west-trending swath of Medussae Fossae Formation materials that occurs along the highland–lowland boundary to the west of the Tharsis Montes shield volcanoes (Scott and Tanaka, 1986; Greeley and Guest, 1987), and the large isolated shield volcano Apollinaris Patera (Scott et al., 1993). The corridor includes the large basins of Elysium and Amazonis Planitiae, which may have been occupied by water bodies (Parker et al., 1987; Scott et al., 1995). These basins are primarily blanketed by stratigraphically young lava flows (e.g., Tanaka et al., 2003, 2005).

The diverse geologic record in the Tharsis/Elysium corridor is dominated by magmatic and tectonic activity and the interaction of magma, basement structures (e.g., joints, fractures, and faults), and liquid water and/or ice, largely linked to the evolution of the Tharsis (Dohm et al., 2001a; Komatsu et al., 2004) and Elysium (Tanaka et al., 1992, 2003, 2005) magmatic complexes. The two complexes are prominent surface expressions related to the concentrated release of internal heat energy during the hypothesized stagnant-lid phase of Mars' evolution (Baker et al., 2007). Incipient development of Tharsis is recorded as far back as the Noachian (Anderson et al., 2001; Dohm et al., 2001a; Solomon et al., 2005), whereas Elysium began to form during the Early Hesperian (Tanaka et al., 2005). Episodic activity has continued for both complexes at least until geologically recent time, well into the Late Amazonian (e.g. Dohm et al., 2001a; Anderson et al., 2001, 2004; Tanaka et al., 2003, 2005).

2.2. Age constraints

Crater density analysis reveals that Mars displays geologic terrain units with formation ages ranging throughout the planet's history (Tanaka, 1986; Barlow, 1988; Hartmann and Neukum, 2001). While Earth and Venus only retain very young surface units and Mercury and the Moon are covered largely by ancient terrain, Mars displays surface units from throughout its evolutional history (ancient Noachian to the very recent Amazonian). Barlow's (1988) Viking-based analysis of impact craters larger than 8-km-diameter found that ~50% of the planet dated from the late heavy bombardment period (Noachian geologic units), ~10% formed near the end of the heavy bombardment period (Early Hesperian terrains), and ~40% formed in the post-heavy bombardment period (Late Hesperian and Amazonian geologic units). Recent results on the origin of impacting objects (Strom et al., 2005) indicates that two populations of impactors, based on different crater size distributions, are responsible for the impact crater record in the inner Solar System. The old population, responsible for the period of Late Heavy Bombardment, which ended about 3.8 Ga ago, originated from the main asteroid belt. It was the result of a catastrophic bombardment of all terrestrial planets due to a sweeping of resonances through the main asteroid belt by migrations of the outer planets (Kring and Cohen, 2002; Gomes et al., 2005). The younger population represents the cratering record from about 3.8 Ga to the present (Strom et al., 2005). This population originated from asteroids that have been perturbed into the inner Solar System when they were moved into resonances by the Yarkovsky effect and then ejected into inner planet-crossing orbits.

In Barlow's (1988) analysis, the youngest geologic units were in the Tharsis region, the Valles Marineris floor deposits, and the polar caps and polar-layered deposits. Tanaka's (1986) analysis of craters larger than 2-km-diameter showed that Tharsis volcanic flows, the polar regions, portions of Arcadia Planitia, and the Cerberus Fossae/Marte Valles region were formed within the past ~700 Ma, during the Late Amazonian period.

Higher resolution imagery available from MOC and THEMIS VIS allow extension of crater density studies to smaller craters and can provide statistically significant results for more localized regions than was available using Viking data. In addition, improved observations of the number of Mars-crossing asteroids and comets have resulted in stronger constraints on the absolute ages of

surface units based on crater density analysis (Neukum et al., 2001; Ivanov, 2001). Hartmann and colleagues have derived crater isochron curves for Mars and have used such plots in determining the ages of terrain units (Hartmann et al., 1999; Hartmann and Berman, 2000; Hartmann and Neukum, 2001). They find that the youngest lava flows on Olympus Mons have ages between 10 and 100 Ma, while the youngest lava flows in Amazonis and Elysium Planitiae are less than 10 Ma old (Hartmann and Berman, 2000; Hartmann and Neukum, 2001). Crater counts in the plains adjacent to Cerberus Fossae suggest recent fluvial activity, in the range of 10–100 Ma (Burr et al., 2002; Berman and Hartmann, 2002), although Plescia (2003) argues for much older ages (144–1700 Ma).

Age determination based on analysis of small craters suffers from a major problem: the contamination of the cratering record by secondary craters. Absolute ages for martian terrain units are derived by extrapolation of the lunar crater chronology, which assumes some ratio of martian to lunar impact flux (Ivanov, 2001). Hartmann's studies generally assume that the secondary crater production rate on Mars is equivalent to that on the Moon and need not be a concern to the resulting age determinations. However, recent studies of martian impact crater ejecta fields have led McEwen et al. (2005) and Barlow (2006) to question this assumption.

The Tharsis–Elysium corridor is an area which has been affected by secondary craters from the formation of the 10-km-diameter crater Zunil (McEwen et al., 2005) and thus the use of small craters to obtain surface ages in this region is suspect. To avoid the contamination from Zunil secondaries, we have conducted crater count analysis for craters $\geqslant$5-km-diameter in selected areas of the southern Amazonis Planitita region (including those that include the Cerberus Fossae, the Medusae Fossae Formation, and the NSVs). Secondary craters are expected to be a minor contributor to the crater record in this diameter range, but the tradeoff is that we must analyze larger areas to obtain statistically significant results. Our results give an average crater density of 5.97×10^{-5} craters $\geqslant$5-km-diameter km^{-2}, which, using the Hartmann isochrons, suggests that these regions display a maximum age of about 1 Ga. Although these results indicate older average ages than the smaller crater analysis, it still confirms that the Tharsis/Elysium corridor contains some of the youngest geologic units on the planet.

2.3. Geologic history

A diverse suite of geologically young (Amazonian) volcanic and water-related landforms are recognized in the Tharsis/Elysium corridor. The stratigraphic positions of rock units in the Tharsis/Elysium corridor were established by previous Viking-based regional and global mapping investigations (e.g., Scott and Chapman, 1991; Morris et al., 1991; Scott et al., 1993, 1995, 1998; Chapman and Tanaka, 1993; Craddock and Greeley, 1994; Zimbelman et al., 1994; Morris and Tanaka, 1994; Scott and Zimbelman, 1995; Tanaka et al., 2003, 2005). The Tharsis/Elysium corridor contains the largest concentration of stratigraphically young (Amazonian) rock materials (volcanic and sedimentary) recorded on the planet (Tanaka et al., 2005; Nimmo and Tanaka, 2005).

Tharsis displays a suite of volcanic landforms of diverse sizes and shapes, including extensive lava flow fields and large igneous plateaus in addition to the well-known constructs. Early volcanic activity in Tharsis included explosive volcanism, but this transitioned into more concentrated volcano and fissure-fed low-viscosity eruptions during the Late Hesperian (Dohm and Tanaka, 1999; Dohm et al., 2001c). Although Tharsis records episodic activity since the Noachian Period (Dohm et al., 2001a), late-stage development of Tharsis Montes and Olympus Mons has occurred during the Amazonian Period and includes the emplacement of associated lavas and aureole deposits (Morris et al., 1991; Morris and Tanaka, 1994; Scott and Zimbelman, 1995; Scott et al., 1998; Neukum et al., 2004). In contrast, Elysium records concentrated magmatism beginning in the Early Hesperian (Greeley and Guest, 1987; Tanaka et al., 2003, 2005) that has resulted in the development of shield volcanoes and the emplacement of lava flows.

Pristine lava flows are observed in the Elysium and Amazonis Planitiae basins, originating from both Tharsis and Elysium volcanic complexes and from fissures (Tanaka et al., 2005) such as those related to large dislocations tens to hundreds of kilometers long in the martian crust (e.g., Dohm et al., 2002a). An example of these fissures is the northwest-trending Cerebus Fossae (Greeley and Guest, 1987; Tanaka et al., 2003, 2005). A possible linkage between Tharsis and Elysium via a complex fabric of crustal/lithospheric faults and fractures cannot be ruled out because these young lava flows bury older rock surfaces, including an ancient basement structural fabric (Tanaka et al., 2005).

Geological mapping indicates that tectonism in the Tharsis/Elysium corridor has continued into the Late Amazonian, albeit to a far lesser and more localized extent when compared to Noachian and Early Hesperian magmatic-driven tectonic activity (Anderson et al., 2001, 2004; Dohm et al., 2001c). Tectonic structures such as fractures, faults, and structurally controlled pit crater chains cut stratigraphically young lava flows and aureole deposits of the Tharsis Montes shield volcanoes (Figs. 3 and 4) and Olympus Mons (Scott and Tanaka, 1986; Mouginis-Mark, 1990; Morris et al., 1991; Morris and Tanaka, 1994; Scott and Zimbelman, 1995; Scott et al., 1998; Wyrick et al., 2004; Ferrill et al., 2004; Márquez et al., 2004), plains-forming materials of Elysium and Amazonis Planitiae (Hartmann et al., 1999; Hartmann and Berman, 2000; Tanaka et al., 2003), and shield-forming lava flows of Elysium (e.g., Greeley and Guest, 1987; Tanaka et al., 1992, 2003, 2005). Thus, tectonism recorded in the Tharsis/Elysium corridor points to an internally active Mars up to

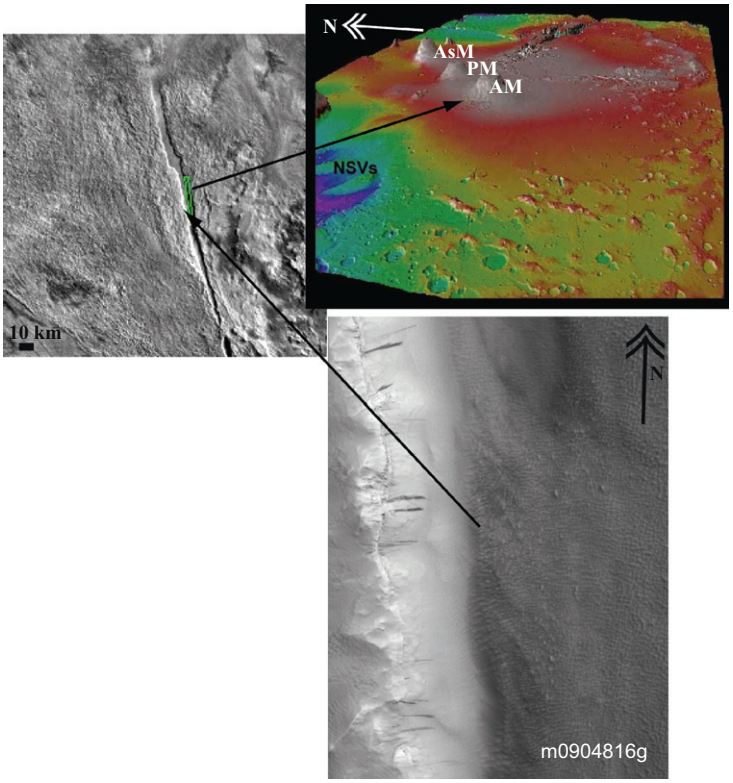

Fig. 3. (Top right) MOLA-based 3D map projection looking northeast across the Tharsis magmatic complex, which includes the NSVs region and the Tharsis Montes shield volcanoes, Arsia Mons (AM), Pavonis Mons (PM), and Ascraeus Mons (AsM). (Top left) Viking context image showing graben, which cuts stratigraphically young (Middle to Late Amazonian) aureole deposits on the northwest flank of Arsia Mons shield Volcano (Scott and Zimbelman, 1995); there is about 1875 km that separate the southwest margin of Arsia Mons from the northeast margin of Ascraeus Mons. (Bottom) MOC image m0904816g showing dark slopes streaks, which occur on the slope of the east-facing fault scarp of the graben (Top left) with few if any impacts observed on the floor of the graben. Width of image is about 3574 m.

recent times with evidence of fluvial activity associated with these areas of recent tectonism. This is consistent with other parts of Mars that appear controlled by the basement structural fabric (e.g., Tanaka et al., 1998; Dohm et al., 2001c).

Tectonism in the Tharsis region consists of fault and rift systems of varying extent and relative formation age. This includes the vast canyon system of Valles Marineris, which is interpreted to be the site of a lithospheric zone of weakness and vertical uplift related to mantle plume impingement at the base of the lithosphere (Dohm et al., 2001a). In addition, Tharsis displays a system of radial faults and circumferential wrinkle ridges and fold belts (Schultz and Tanaka, 1994), which are centered about local and regional centers of tectonism, interpreted to be the result of plume-driven uplift (Anderson et al., 2001a). Tectonic activity associated with the development of Elysium is far less extensive in time and space than for Tharsis (Anderson et al., 2007b, in review).

The Medusae Fossae Formation forms a broad but discontinuous band of wind-etched materials trending east-west along the dichotomy boundary (e.g., Scott and Tanaka, 1986; Greeley and Guest, 1987; Scott and Chapman, 1991) which was emplaced during the Middle to Late Amazonian. On the basis of its morphologic characteristics, the Medusae Fossae Formation has been interpreted to consist of ash-flow tuffs (Malin, 1979; Scott and Tanaka, 1982, 1986), ancient polar deposits (Schultz and Lutz, 1988), or pyroclastic and eolian materials (Greeley and Guest, 1987). Channels and other types of valley forms, some of which appear to be structurally controlled, dissect the stratigraphically young materials of the Medussae Fossae Formation in places (e.g., Scott and Chapman, 1991; Scott et al., 1993, 1995) (Fig. 5), indicating fluvial activity along the highland–lowland boundary extended well into the Amazonian Period.

The history of the allocation, transportation, and deposition of water on Mars is of great importance to interpreting its geologic history. While Earth is a hydrologically active world punctuated by Ice Ages, Mars is a frozen world punctuated by periods of warming and hydrologic activity (Baker, 2001; Fairén et al., 2003). Particlarly, Tharsis is characterized by five major pulses of magmatic-driven activity that decline in areal and temporal extent with time and that interact with an ancient basin and productive aquifer system to form outflow channel systems (Dohm et al., 2001a, 2007a; Baker et al., 2007) and possible water inundations in the northern plains (Fairén et al., 2003). Such long-term interaction of endogenic-driven activity and water collectively point to

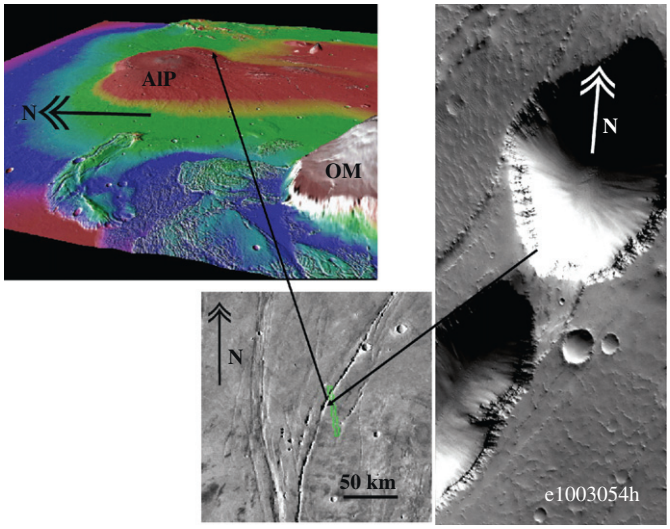

Fig. 4. (Top Left) MOLA-based 3D map projection looking across the northwest flank of Olympus Mons (OM) and Alba Patera (AlP); there is about 1850 km that separate the summit region of Olympus Mons and the summit region of Alba Patera. (Bottom left) Viking context image showing both structurally controlled pit crater chains (e.g., Wyrick et al., 2004), which cut Amazonian lava flows of the large shield complex, Alba Patera (Anderson et al., 2004), and location of MOC image e1003054h (right). The MOC image shows pristine collapse structures along faults with very little infill and few if any impact craters. Again, the boundary of the corridor is approximately located, and as such, could possibly be expanded to include Alba Patera. Width of image is about 3064 m.

Tharsis (including Elysium) as a prime target for ancient and possibly extant hydrothermal environments (Schulze-Makuch et al., 2007). The Tharsis/Elysium corridor provides a diverse record of episodic hydrologic events (also see Table 1), including:

- Noachian–Early Hesperian NSVs outflow channel flooding. The NSVs represent the northwest watershed of Tharsis, whereas the circum-Chryse outflow channel system is the northeast watershed (Dohm et al., 2001a, b).
- Noachian–Hesperian (and possibly Amazonian) magma–water interactions associated with the development of the prominent shield volcano, Apollinaris Patera (Scott et al., 1993).
- Late Hesperian–Early Amazonian Mangala Valles outflow channel flooding (Chapman and Tanaka, 1993; Craddock and Greeley, 1994; Zimbelman et al., 1994).
- Late Hesperian–Amazonian sapping valley formation in the Mangala Valles/NSVs regions (Dohm et al., 2001b, 2004).
- Hesperian/Amazonian magma-driven flooding in and near Elysium, such as at structurally controlled valley systems of Galaxis Fossae (Mouginis-Mark, 1985; Greeley and Guest, 1987; Tanaka et al., 2003).
- Amazonian flooding to form Marte Vallis, a reported spillway that connected the putative Elysium and Amazonis paleolakes (Scott et al., 1995), as well as sites of possible earlier oceans (e.g., Parker et al., 1993; Fairén et al., 2003).
- Amazonian structurally controlled flooding located to the east of Olympus Mons (Mouginis-Mark, 1990) (Fig. 6).
- Amazonian hydrologic activity observed locally along the highland–lowland boundary west of Tharsis Montes, such as the stratigraphically young valleys that dissect Middle to Late Amazonian Medusae Fossae Formation materials (Scott and Chapman, 1991; Scott et al., 1993, 1995; Dohm et al., 2004).
- Present-day formation of anastomosing dark streaks that occur on hillslopes of the Mangala Valles/NSVs region, which may be another indicator of local aqueous activity (Ferris et al., 2002; Miyamoto et al., 2004), though dust avalanching is also a viable formation mechanism for many of the streaks (Sullivan et al., 2001).

Elysium and Amazonis Planitiae have been hypothesized to have contained bodies of water ranging in size from oceans (Parker et al., 1993) to lakes (Scott et al., 1995). These basins are partly covered by stratigraphically young lava flows that source from Tharsis, Elysium, and structurally controlled fissures like Cerebus Fossae (Tanaka et al., 2003) (Fig. 7). Magmatic-tectonic-water activity at Elysium continued well into the Amazonian Period, as evidenced from the lahar-like flows that source from Elysium and extend into the Utopia basin to the northwest (Mouginis-Mark, 1985; Tanaka et al., 2003, 2005; Russell and Head, 2003).

Landforms closely resembling glacial, fluvial, lacustrine, periglacial, and mass-movement features on Earth are observed in parts of the Tharsis/Elysium corridor. On Earth, these features are commonly produced by processes requiring a relatively dense atmosphere and related transport and precipitation of water (Baker, 2001). The martian analogs include the aureole deposits occurring on the northwest flanks of the Tharsis Montes shield volcanoes and Olympus Mons. The aureole deposits display at least three different facies (e.g., ridged, knobby, and smooth), all of which may indicate stratigraphically recent magma–water interactions and glacial/ice sheet/rock glacier activity (e.g., Scott and Zimbelman, 1995; Scott et al., 1998; Head et al., 2003a, 2005, 2006; Shean et al., 2005; Milkovich et al., 2006). If glacial in origin, the aureole deposits would require substantial transport of atmospheric water vapor to sustain a positive net mass balance through snow accumulation. The period during which the hypothesized glaciers grew and advanced would have been followed by the change to present-day conditions, such that ice wasted back to relict rock glaciers and probable debris-mantled relict ice (Baker, 2001). In addition to the aureole deposits, evidence of Amazonian magma–water interactions in the Tharsis/Elysium corridor include sapping channels, structurally controlled valley forms, anastomosing dark slope streaks (Fig. 8), erosional scarps, and lahar-like flows (Mouginis-Mark, 1985, 1990;

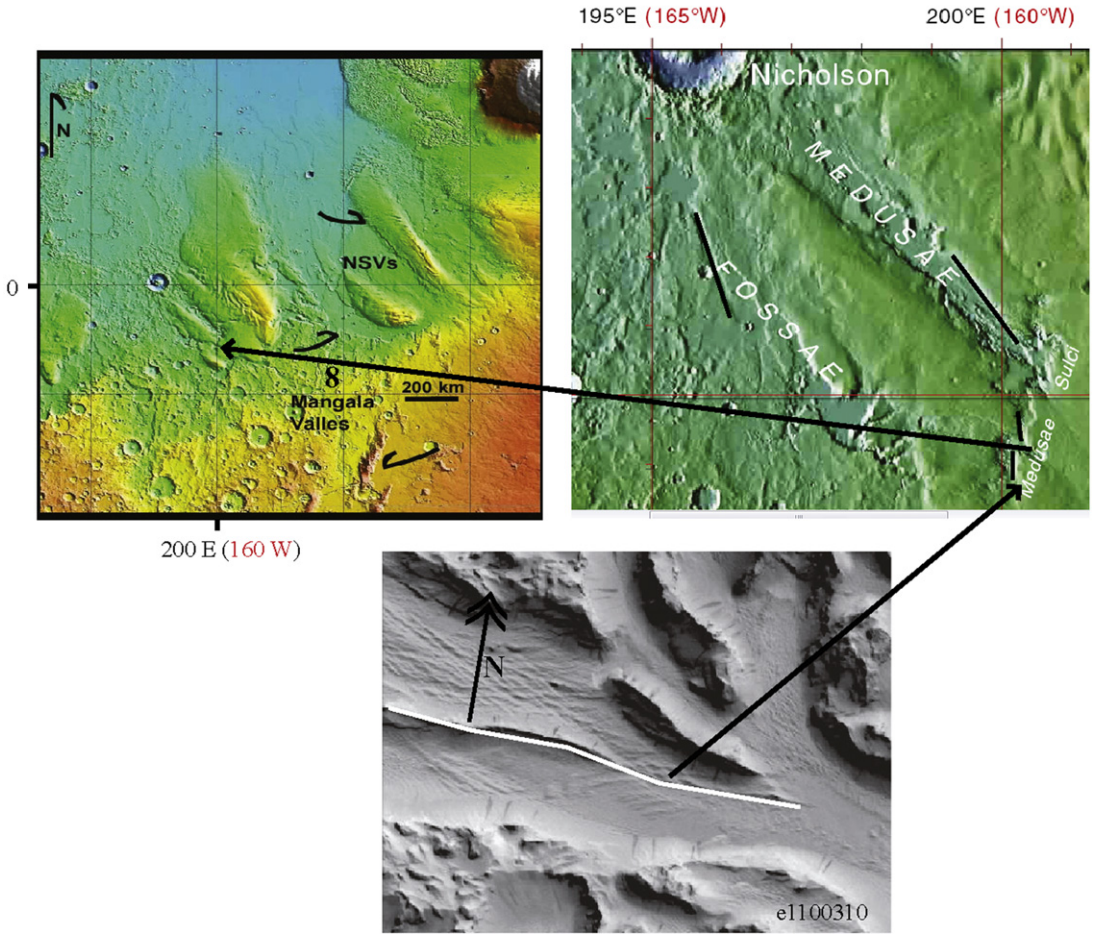

Fig. 5. (Top left) MOLA topographic map showing the NSVs and Mangala Valles regions (based in part on Dohm et al. (2001a, b, 2004). Large arrows (from south to north) indicate headwaters of Mangala Valles, debouchment region of northeast part of Mangala Valles, and central part of the NSVs, and the approximate location of MOC m1101809 of Fig. 8 is shown. (Top right) MOLA image showing Medusae Fossae. Note that in addition to wind erosion along the Medusae Fossae (examples of faults are indicated by thin black lines), possible fault-controlled aqueous activity (e.g., faults as conduits for the migration of water) may have also contributed to the resurfaced landscape. (Bottom) MOC image e1100310 shows valleys dissecting Medusae Fossae Formation materials possibly resulting from fluvial activity, tectonism (e.g., white line marks an inferred fault), and/or wind erosion. Width of image is about 3057 m.

Scott et al., 1995; Ferris et al., 2002; Tanaka et al., 2003; Dohm et al., 2004).

These landforms are anomalous under the very cold and dry present-day martian conditions, but may be explained by one or more short-duration ($\sim 10^3$–10^4 years) episodes of environmental change occurring since about 10^7–10^8 years ago (Head et al., 2003a, 2005, 2006; Milkovich et al., 2006), possibly triggered by locally extensive volcanism and associated outburst flooding of groundwater (Baker, 2001). Variation of martian orbital parameters (e.g., Carr, 1990; Touma and Wisdom, 1993; Laskar and Robutel, 1993; Shean et al., 2005) also may have contributed to the geomorphic expression recorded within the Tharsis/Elysium corridor. Over the past 10 Myr, obliquity values have varied from as low as 15° to as high as 50° (Touma and Wisdom, 1993; Laskar and Robutel, 1993), and more recent work by Laskar et al. (2004) indicates the most probable obliquity over the past 4 Gyr has been 45°. Mischna et al. (2003) modeled the water cycle using a global circulation model and found that water ice migrates to the tropics during periods of high obliquity (>40°). More recent work (Abe et al., 2005) indicates that, with wet surface conditions, the precipitation can concentrate in the equatorial zone at obliquities greater than 30°. Similar modeling has also shown that, under current surface pressure and obliquity conditions, there exists the potential for transient liquid water to form in the Elysium/Tharsis corridor because of the large diurnal range of surface temperatures (Richardson and Mischna, 2005).

Touma and Wisdom (1993) proposed that an obliquity >30° would generate an atmospheric pressure above 25 mbar, allowing a total water release to the atmosphere equivalent to 500 pr μm (equivalent surface thickness as water) (Jakosky and Carr, 1985). Environmental conditions conducive to the formation of the aureole deposits, sapping channels, structurally controlled valley forms, dark slope streaks, erosional scarps, and lahar-like flows would be enhanced when such obliquity conditions were coupled

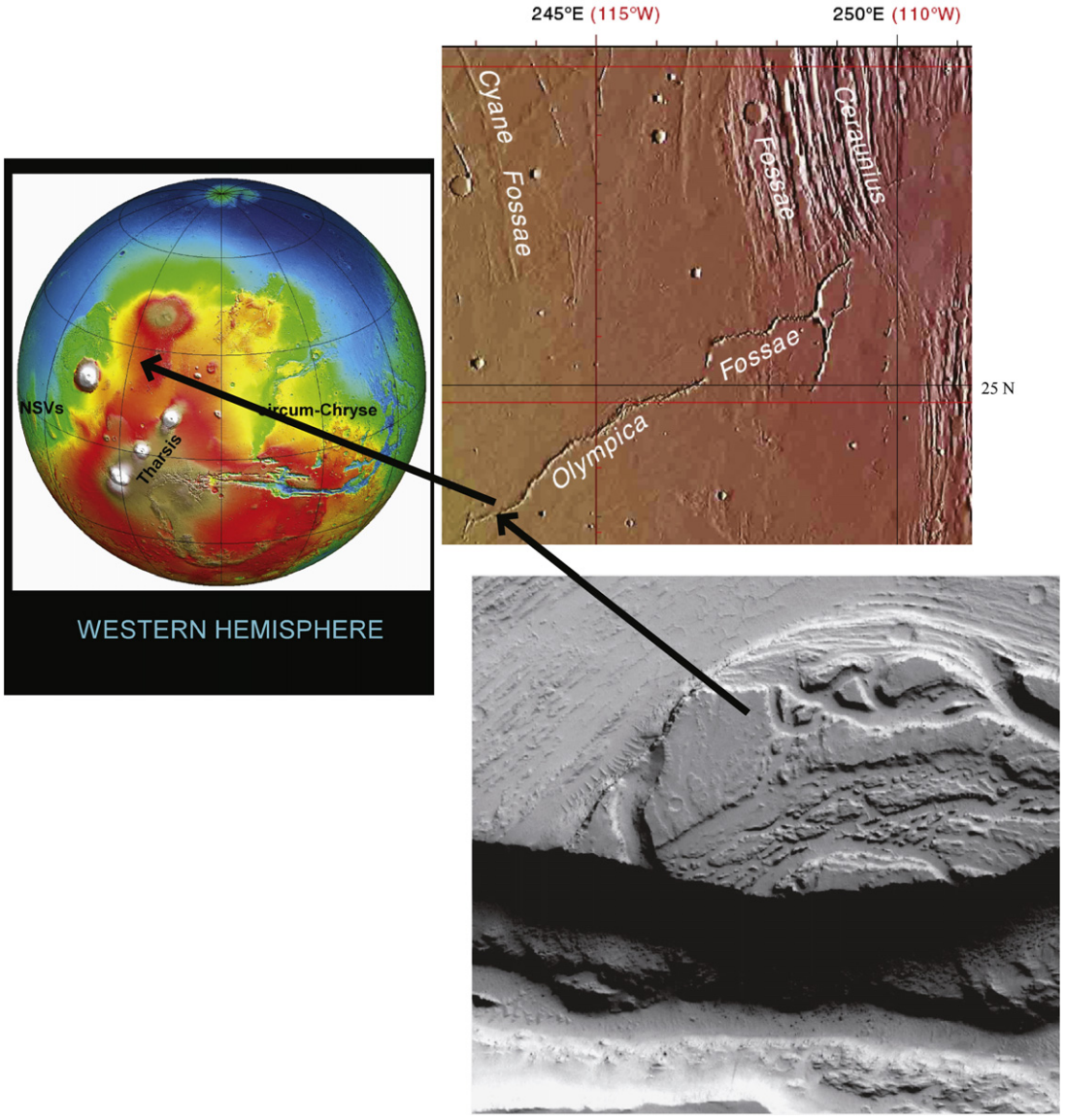

Fig. 6. (Top left) MOLA topographic map of Tharsis magmatic complex highlighting the northeast-trending chain of gigantic shield volcanoes, Tharsis Montes, and the northeast and northwest watersheds of Tharsis, circum-Chryse and northwestern slope valleys (NSVs), respectively (Dohm et al., 2001a, b). (Top Right) MOLA image showing structurally controlled fluvial activity among Olympica Fossae located to the east of Olympus Mons (e.g., Mouginis-Mark, 1990) dissecting Amazonian lava flow materials (Scott and Tanaka, 1986). (Bottom; north is at top) MOC image e1002900 showing faulted and flood-carved terrain, which include streamlined bedforms and few impact craters. Width of the image is about 3748 m.

with Tharsis-induced activity. Therefore, obliquity provides a mechanism for accumulating water ice in the region and lends additional support to the newly emerging paradigm of a water-rich Mars, which may be active well into the future in regions such as the Tharsis/Elysium corridor.

3. Compositional evidence of a potentially internally active Mars

An internally active Mars is further supported by compositional evidence, including martian meteorite and remote sensing mineralogic analyses.

3.1. Martian meteorites

Martian (SNC) meteorites provide clear evidence for relatively recent igneous activity on Mars. Isotopic analysis of shergottites indicates that Mars differentiated rapidly, forming the core and the mantle source regions of the SNCs within a few tens of million of years after planetary accretion (Brandon et al., 2000; Borg et al., 2003). All of the martian meteorites except ALH84001 crystallized in lava flows or other shallow magma bodies during Amazonian times (see Borg et al., 2003). Excluding ALH84001, the nakhlites are the oldest of the martian meteorites, with crystallization ages of 1.3 Ga, too old to infer much about the possibilities for very recent activity on

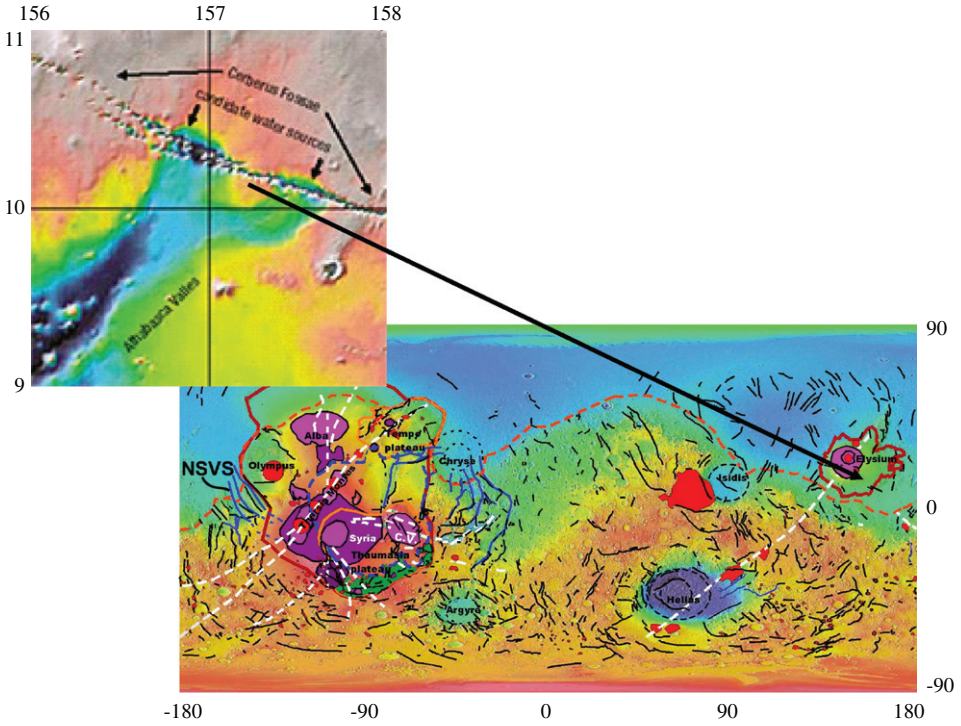

Fig. 7. (Top left) MOLA-based graphic showing geologically recent floodwaters, which source from faults of Cerberus Fossae near the southeastern margin of the Elysium rise volcanic province. The floodwaters, hypothesized to result from the interaction of magma, water, and faults, carved Athabasca Valles perhaps within the last few million years (Burr et al., 2002; Mitchell and Wilson, 2003; Head et al., 2003b), activity of which was followed by the emplacement of lava flows (Jaeger et al., 2007), possibly subduing evidence of hydrated minerals (graphic based from Mitchell and Wilson, 2003). (Bottom right) MOLA-based macrostructures (tectonic structures tens to thousand of kilometers long; revised from Dohm et al. (2002a). Most macrostructures are interpreted to result from pre-Tharsis superplume plate tectonism (e.g., Baker et al., 2002, 2007, Dohm et al., 2002a; Fairén and Dohm, 2004), giant impacts (e.g., Chryse, Utopia, Argyre, Hellas, Isidis, and possibly Arabia Terra (see Dohm et al., Icarus—(2007)), and the development of Tharsis (Dohm et al., 2001a, 2002b, 2007b) and Elysium (e.g., Greeley and Guest, 1987; Tanaka et al., 2005), both of which may be linked by basement structures including Cerberus Fossae (faults and fractures may be buried, in places, by lava flows and sedimentary deposits). Tharsis superplume (Baker et al., 2007; Dohm et al., 2007a) and Elysium rise (red lines), highland–lowland boundary (orange dashes), structural weakness in crust/lithosphere (white dashes), extensional, thrust, and/or transform faults (black lines), Tempe and Thaumasia igneous plateaus (orange lines), Thaumasia highlands and Coprates rise mountain ranges (green patterns), magmatic-driven structural landform complexes of Tharsis superplume (irregular shapes colored in varying shades of violet—see Dohm et al. (2001a) for relative age of formation), promontories, which are interpreted to be shield volcanoes, silicic-rich lava domes (e.g., andesitic domes), highly degraded intrusives, and impact-related massifs (red quasi-circular patterns), outflow channels (blue lines), and Tharsis superplume basin/aquifer system (dashed blue line).

Mars. However, all the shergottites have crystallization ages <500 Ma, with eight in the range 165–180 Ma, one having an age of 327 Ma, and two displaying ages of about 475 Ma (McSween, 2002). These data, although far from a representative sampling of martian volcanic deposits, suggest intermittent magmatism during the past 500 Ma. Eruptions more recent than the formation of the youngest shergottite (165 Ma) could have occurred on Mars as well. Unfortunately, because the SNC meteorites do not provide a representative sampling of the surface, we cannot use the age data to infer how magma flux has varied during the past 1 Ga.

Martian meteorites also inform us about weathering events during the past several hundred million years. All contain small quantities of alteration products (McSween and Treiman, 1998; Bridges et al., 2001) that formed on Mars. Samples of smectite-iron oxide mixtures (iddingsite) from the Lafayette nakhlite give K–Ar ages of between 0 and 650 Ma ago, which might indicate intermittent formation of alteration products during this time (Swindle et al., 2000). Weathering products in the shergottites have not been dated, but they clearly formed after the rocks crystallized in their parent lava flows, so aqueous alteration must have occurred as recently as the age of the youngest shergottites, 165 Ma. Considering the limited number of martian meteorites, it seems likely that aqueous alteration events have occurred more recently than 165 Ma.

3.2. *Mars Odyssey GRS elemental information*

MO's GRS instrument is providing evidence of substantial elemental differences across the surface of Mars (Boynton et al., 2002, 2004, 2007). The GRS instrument is sensitive to elemental compositions within a few tens of centimeters below the martian surface and is capable of cutting through any thin layers of dust that may be present. GRS data reveals that the surface is far from homogenous, with distinct elemental signatures across all regions of

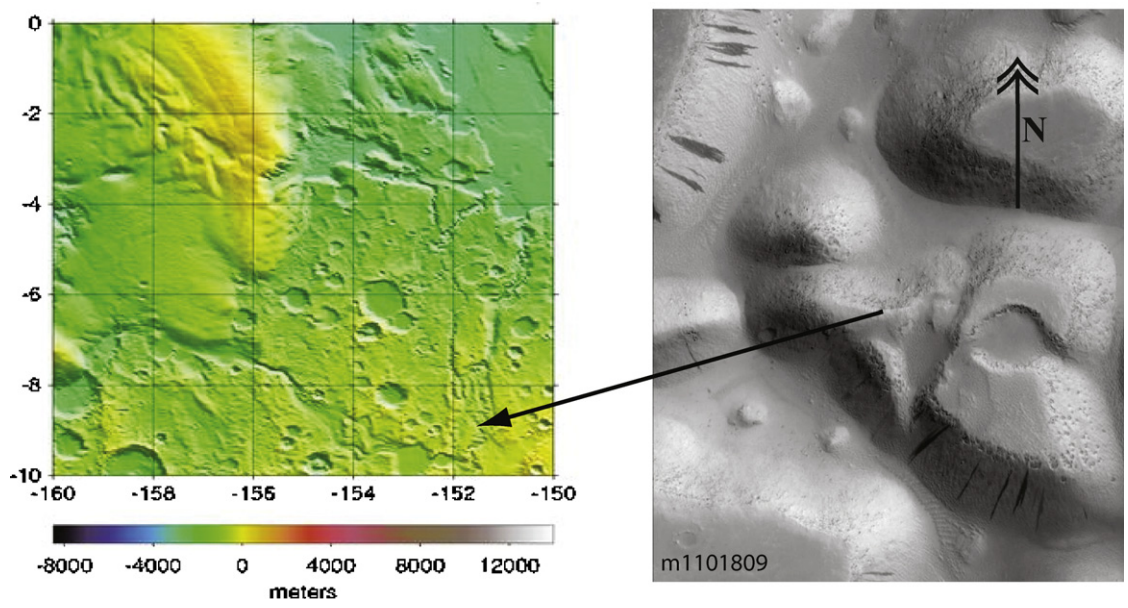

Fig. 8. (Left) MOLA map showing Mangala Valles (also see context image of Fig. 5). (Right) MOC image m11101809 shows numerous darks slope streaks occuring on the hillslopes of Mangala Valles outflow channel system; slope streaks have been identified in the corridor and Arabia Terra regions and parts of Tharsis outside of the corridor region through analysis of MOC data (see Fig. 2 adapted from Rifkin and Mustard, 2001, showing concentrations of streaks). The dark slope streaks often appear to source from geologic contacts. One explanation is dust avalanching (Sullivan et al., 2001), while water as an agent cannot be ruled out (Ferris et al., 2002), especially for the anastomosing-patterned streaks (Miyamoto et al., 2004). Width of image is about 2923 m.

Mars (both with respect to variations in a single element and with respect to establishing correlations or differences between elements). The presence of dust layers contributes to the GRS signal, so what the GRS "sees" is the averaged effect of vertical dust and rock stratigraphy. An important question that arises, therefore, is whether any elemental abundance variations are simply due to changes in mobile dust/rock areal abundance ratios. Based on a multivariate correlation analyses, Karunatillake et al. (2006) argue that dust/rock variations are not key factors in the fluctuation of elemental wt% over the surface. When compared to other parts of Mars, the Tharsis/Elysium corridor records elevated elemental abundances including water (GRS detects H, not H_2O or OH; nevertheless, for uniformity throughout this paper, we report H_2O equivalent wt% computed from H concentrations) and Cl (top and bottom of Fig. 9, respectively).

The technique for determining elemental abundances from GRS data is detailed in Boynton et al. (2002, 2004, 2007). GRS data collected between June 2002 and April 2005 are presented in Boynton et al. (2007), summed into both gridded and regional data products. Gridded data can be smoothed using various filters in an attempt to improve signal-to-noise and to better simulate the large footprint size of the GRS detector, which at the equator is a circle with a radius that varies as a function of energy between 360 and 480 km. Given the nature of GRS data, it is important to focus on large-scale differences over large continuous regions of the planet.

Another means of improving signal-to-noise involves summing over larger regions. Fig. 10 provides regional data for various elements summed over the corridor region and normalized to the remainder of the planet surface excluding the polar regions (see Boynton et al., 2007, in press, for more information on regional summing techniques). These values were obtained by taking an equal area average of concentration values for 5°- × -5° grids within each region. This figure shows that the corridor region is elevated in both H and Cl and depleted in silicon (Si) and potassium (K) compared to the rest of Mars.

The composition of the surface varies throughout the corridor, a clear indication of the complexity of the geologic processes that shaped it. However, the distribution of some elements suggests that the composition may have been affected by recent geologic processes. Cl is particularly enriched in the Medusae Fossae materials (Boynton et al., 2007; Keller et al., 2006), a major geologic formation in the Tharsis/Elysium corridor. There are several likely contributors to this striking enrichment (Keller et al., 2006) and they may all have operated to a greater or lesser extent. One possibility is the reaction of the fine-grained volcanic materials of Medusae Fossae with acid-fog emissions from either the Tharsis volcanoes or from other local source vents that may have since been erased or buried. The elevated H_2O contents in this region are consistent with this mechanism. Cl- and H-rich deposits suggest either recent volcanic activity or continuous erosion to expose fresh, Cl-rich hydrated minerals, water/water ice, interstitial brine solutions, –OH radicals (as in jarosite), or a combination of all. While exposure of previously buried Cl-rich deposits through aeolian erosion is probable, it is also possible that a recently active hydrologic system has

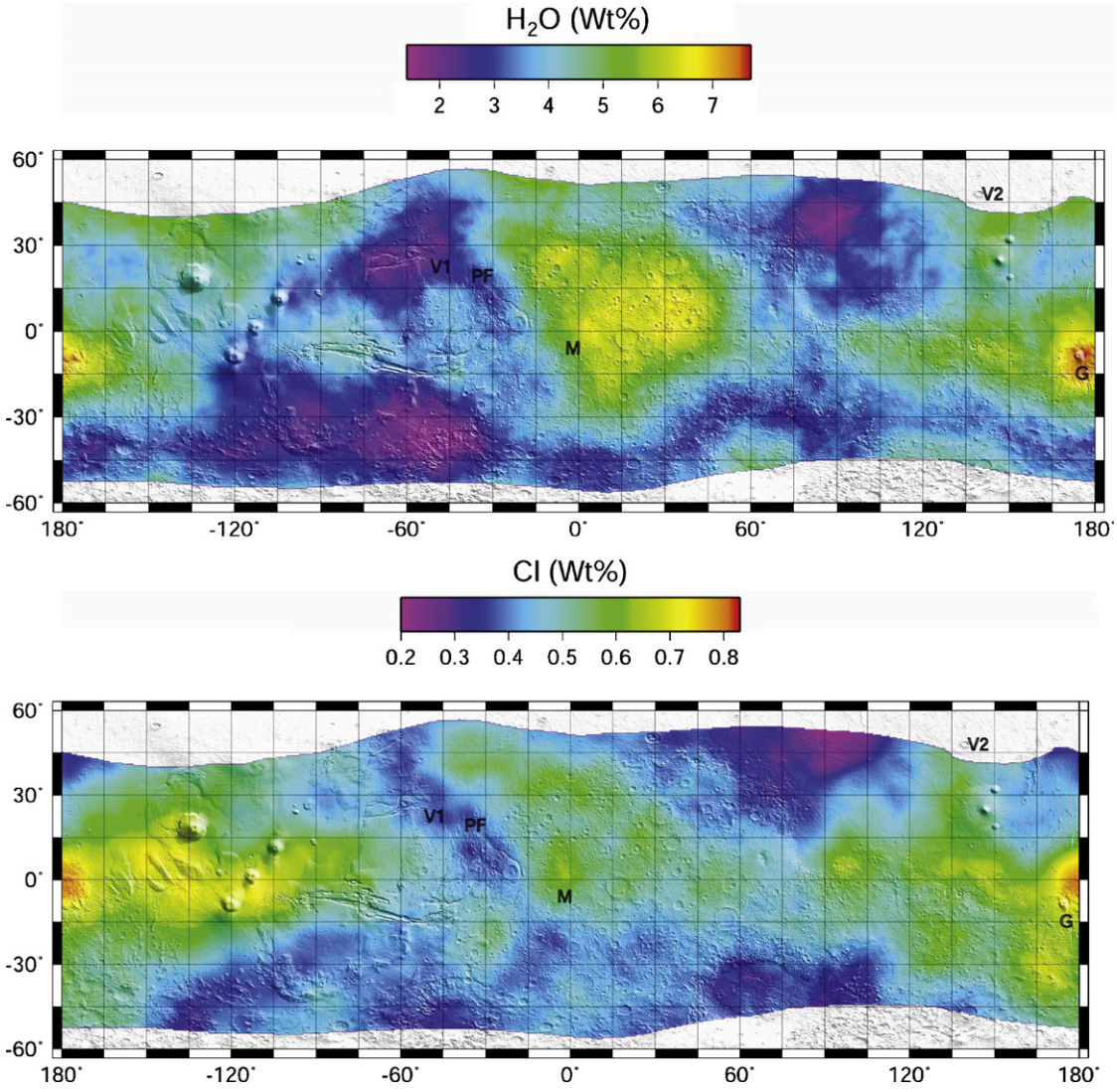

Fig. 9. Anomalous elevated H_2O (top) and Cl (bottom) concentrations in the Tharsis/Elysium corridor region (e.g., Boynton et al., 2002, 2004, JGR—2007; Feldman et al., 2002) may indicate possible aqueous activity related to the interactions of magma with water/water ice and fluvial activity, as well as other contributors such as acid fog (see Keller et al., 2006). V1, V2, PF, M, and G denote the general locations of the Viking 1, Viking 2, Mars Pathfinder, Opportunity, and Spirit.

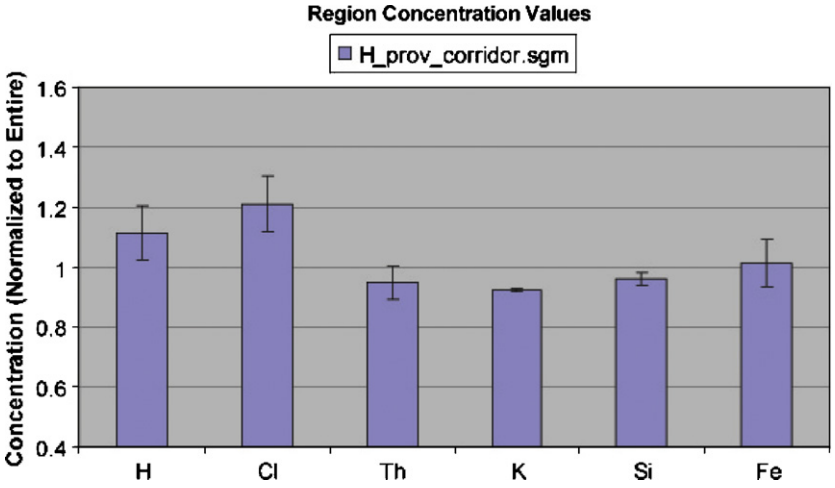

Fig. 10. Elemental enrichment factors for H, Cl, Th, K, Si, and Fe, determined using gamma ray sums for the corridor region. Concentration values have been normalized to the average concentration of the equatorial regions. Note that both H and Cl are elevated.

eroded some of the original material of the Medusae Fossae Formation or remobilized Cl from evaporite deposits, contributing to the Cl-enrichment seen by GRS. Remobilization results in transport of some elements to new locations, producing a positive anomaly in the deposition zone compared to the depleted zone. Liquid water is an effective mechanism by which elements can be laterally transported and concentrated. Thus, the elemental data are consistent with a combination of volcanic acid–fog interactions with surface materials, coupled with redistribution by subsequent aeolian and aqueous processes, possibly including hydrothermal activity. In addition, areas of lower Cl concentrations in parts of the corridor region may be explained by the occurrence of Amazonian flow materials, interpreted to be stratigraphically young basaltic lavas (e.g., Scott and Tanaka, 1986; Greeley and Guest, 1987; Morris et al., 1991; Morris and Tanaka, 1994; Tanaka et al., 1992, 2003, 2005; Scott and Zimbelman, 1995; Scott et al., 1998), which are less likely to retain a Cl signature at the upper horizon of the surface under aqueous conditions.

3.3. Remote sensing mineralogic evidence

Recent spectroscopic data are revealing Mars to be a more geologically diverse planet then has been previously reported, revealing evidence of quartz, sulfates, and clays in addition to basalt (e.g., Rieder et al., 2004; Poulet et al., 2005; Christensen et al., 2005; Gendrin et al., 2005; Bibring et al., 2006). The MEx Omega instrument has detected clays, sulfates, and anhydrous ferric oxides at the surface of parts of Mars (Poulet et al., 2005; Bibring et al., 2006), particularly outside of the corridor region. However, both the MGS Thermal Emission Spectrometer (TES) and MEx Omega instruments indicate relatively bland spectral signatures in the Tharsis/Elysium corridor region, interpreted to be mostly a reflection of dust, including Omega-based non-mafic signatures corresponding to ferric oxide signatures (Bibring et al., 2006). This orbital-based spectroscopic information is contrary to other lines of evidence presented above that point to a far-reaching record of magma–water interactions, including potential diverse rock compositions.

Is such a potentially diverse rock record in the Tharsis–Elysium corridor region obscured to orbital-based spectrometers by find-grained materials such as dust or from aqueous (including hydrothermal) alteration in the form of mineral precipitates, or both? A clue to this query may lie near the south-central margin of the corridor region where field-based analysis in Gusev Crater through MER Spirit has revealed elevated chlorine consistent with GRS information (Keller et al., 2006) and a diversity of rock types including sulfates that could be related to hydrothermal activity (one of several interpretations; e.g., see Wang et al., 2007). Apollinaris Patera and surrounding regions located to the north of Gusev is also elevated in chlorine (Keller et al., 2006) and has several features that point to a long-lived history of magma–water interactions (Scott et al., 1993; Schulze-Makuch et al., 2007). Such information coupled with other diverse evidence of ancient and possibly extant magmatic-driven activity (Table 1) underscores the significance of continued MRO data acquisition of the corridor region, including data from the High Resolution Imaging Science Experiment (HIRISE), which provides detailed images (0.25–1.3 m/pixel) (McEwen et al., 2007), and the Compact Reconnaissance Imaging Spectrometer for Mars (CRISM), which images a region approximately 10 km × 10 km at full spatial resolution (15–19 m/pixel) and spectral resolution (544 channels covering 362–3920 nm) (Murchie et al., 2007).

4. Thermal evolution of the Tharsis/Elysium corridor

Both Tharsis and Elysium may result from plumes of diverse dimensions and origins ranging from superplumes (e.g., Maruyama, 1994; Dohm et al., 2002b, 2007a, Li et al., 2003; Baker et al., 2007) to mantle plumes (e.g., Mège and Ernst, 2001). Plumes are an integral part of the internal dynamics of terrestrial planets and have profound influences on surface and subsurface geology and hydrology over long time scales (Komatsu et al., 2004). They can significantly alter large-scale topography, drainages, landscapes, sedimentation, and even climate (Baker et al., 1991, 2002; Maruyama, 1994; Li et al., 2003; Komatsu et al., 2004). Both Tharsis and Elysium are extremely significant in the thermal evolution of Mars, especially during the purported stagnant-lid phase, which has persisted for more than 3.5 Ga. (Fairén and Dohm, 2004). The geologic, elemental, and mineralogic evidence presented above suggests that activity related to the formation of the two complexes occurred well into the Late Amazonian, possibly extending to within the last few million years (Hartmann et al., 1999; Neukum et al., 2004), and collectively point to the Tharsis/Elysium corridor as a region where elevated heat flow and related near-surface aquifers may exist at the present.

4.1. Thermal signatures

If the Tharsis/Elysium corridor is a region of geothermal activity at the present time, why has THEMIS not detected a thermal anomaly in this region? Detection of thermal emission resulting from volcanic or geothermal activity on Mars would be one of the greatest discoveries of planetary exploration. To determine if such a detection is likely to be made, we consider two possible manifestations of volcanic activity on the martian surface that may be detected by instruments on remote sensing platforms. The first results from the emplacement of high-temperature silicates, such as basalt, which typically erupts at temperatures in excess of 1400 K. Effusive volcanic activity will result in hydrothermal activity through interaction with the martian cryosphere. The second process is hydrothermal activity where water in the cryosphere is mobilized by intrusive

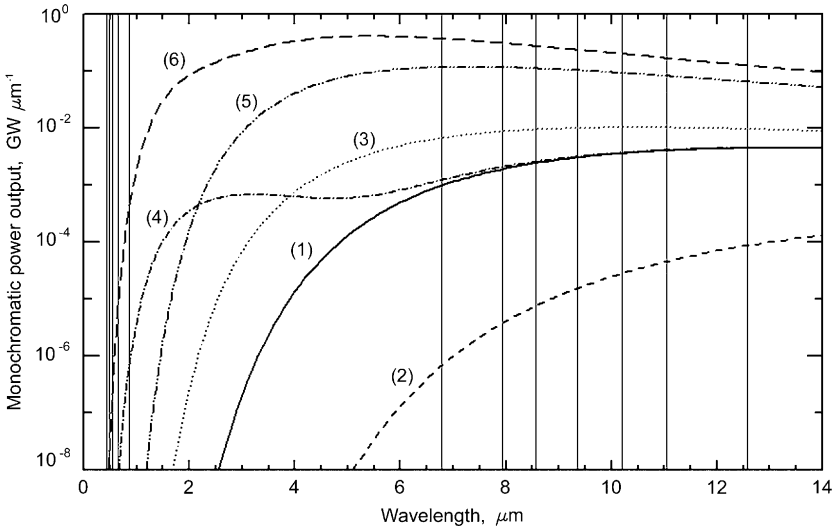

Fig. 11. Thermal emission as a function of wavelengths for different volcanic scenarios on Mars. Each case represents a square kilometer of the martian surface. An emissivity of 0.8 is used except for active silicates, where an emissivity of 0.9 is used. Curves are as follows: (1) solid line = average Mars background at 213 K; (2) short dashed line = polar region at 123 K; (3) dot-dot line = hydrothermal scenario with 0.75 of the area at 213 K and 0.25 at 313 K; (4) dash-dot-dash line = 0.9999 of area at 213 K (background temperature), plus 0.0001 of the area at 900 K (a small area of active silicate volcanism); (5) dash-dot-dot-dash line = recently active silicate area at 400 K; and (6) long dashed line = extensive current silicate activity with 0.99 of the area at 500 K and 0.01 at 1000 K. Vertical lines are the five THEMIS VIS bands (0.425–0.860 μm) and seven IR bands (6.78–12.57 μm).

magmatic activity. Mars's atmospheric pressure is ~1% that of Earth, and water boils at ~313 K at the surface as a consequence of the low water vapor partial pressure (Carr, 1996). If heated to greater temperatures, water will generate steam explosions at the surface.

The chances of detecting either silicate or hydrothermal activity from their thermal emission depend on the temperature and areal distribution of the geothermal source and the wavelength and sensitivity of the instruments on remote platforms. THEMIS (Christensen et al., 2004), the imaging spectrometer on Mars Odyssey, obtains data at five visible bands from 0.425 to 0.860 microns (μm) and ten infrared bands from 6.78 to 14.88 μm. The martian atmosphere is opaque to infrared radiation at 14.88 μm, so this band is not used here. The VIS subsystem has a resolution of 19 m/pixel while the IR subsystem has a resolution of 100 m/pixel. Spectral coverage and spatial resolution is sufficient to detect thermal anomalies on the surface of Mars if the area is great enough and the resulting pixel brightness temperature is high enough.

Fig. 11 shows Planck black-body plots for different scenarios of possible active silicate volcanism and hydrothermal activity. Thermal emission curves are plotted for martian background (thermally non-active) pixels and for low-temperature (hydrovolcanic) and high-temperature (basaltic volcanism) cases, with different areas of a THEMIS pixel containing various combinations of areas at different temperatures. Fig. 12 shows the thermal emission for a hydrothermal scenario (line 1) and a silicate scenario (lines 2 and 3) normalized to the martian background. Ratios are shown in Table 2. If active silicate volcanism occurs on a scale greater than a few hundred square meters (for example, coverage by pahoehoe or aa

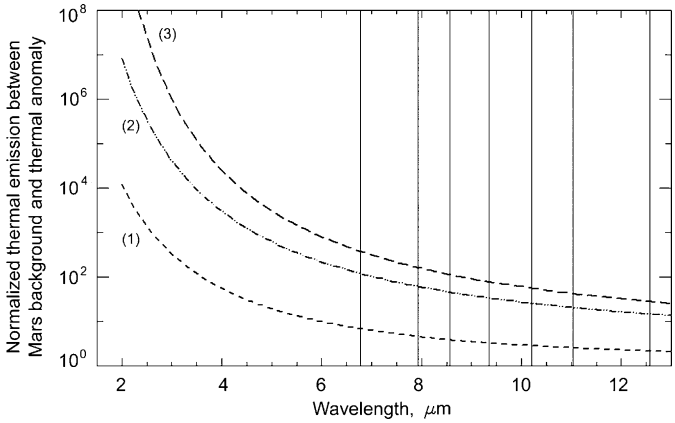

Fig. 12. Thermal emission curves as a function of wavelength normalized to Mars average background emission. (1) Small-dashed line = hydrothermal scenario with 0.75 of the area at 213 K and 0.25 at 313 K; (2) dash-dot-dot-dash line = recently active silicate area at 400 K; (3) long-dashed line = extensive silicate activity with 0.99 of the area at 500 K and 0.01 at 1000 K. THEMIS IR bands from 6.78 to 12.57 μm are shown (vertical lines).

flows), thermal emission is seen across all wavelengths at intensities that are orders of magnitude greater than the martian background. The difference between non-active background and a thermal anomaly is greater than 10 at most wavelengths and may exceed 300 for active volcanism filling most of a pixel (observed at 6.78 μm).

As shown in Figs. 11 and 12, thermal emission from high-temperature silicate volcanic activity would be detected by THEMIS-like instruments, if such activity is taking place and the instrument is fortunate enough to observe this particular location at the right time (at night

Table 2
Ratios of thermal emission normalized to Mars background for different volcanic scenarios (from Fig. 12)

Wavelength (μm)	Hydrothermal activity (1)	Warm silicates (2)	Active silicates (3)
6.78	6.73	117.54	370.20
7.93	4.47	58.92	156.13
8.65	3.75	43.09	105.88
9.35	3.25	33.07	76.31
10.21	2.80	24.86	53.71
11.04	2.52	20.09	41.36
12.57	2.17	14.57	27.90

The relative areas of the "hydrothermal" and "silicate" areas are described in the caption of Fig. 12. Numbers in brackets refer to the scenarios described in the Fig. 12 caption. "Warm" silicates refer to recently erupted lava which exhibits cooled crust. "Active" silicates are lava in the process of being erupted, where areas close to magma eruption temperature are present.

or preferably just before dawn). In the case of hydrothermal activity, no purely thermal detection can be made at visible wavelengths. The thermal emission from a boiling lake would not be distinguishable from background, although visual identification of a plume would suffice for detection in daytime observations. Detection of hydrothermal activity using thermal IR is very difficult due to the relatively low temperatures (Table 2). Hydrothermal activity within a THEMIS pixel, with 0.25 of the pixel area at 313 K emits over 6 times the thermal emission from a non-active pixel at 6.8 μm, but only 2.1 times the non-thermal emission at 12.6 μm. If an entire 100×100 m THEMIS pixel is at 313 K, these differences increase by roughly a factor of 4.

These thermal emission curves have to be modified to account for absorption effects by the martian atmosphere. Quantifying this process is non-trivial as the degree of modification depends on the water ice and dust content of the atmosphere, which are functions of both time of year and latitude/longitude (Smith et al., 2003). One method is to take pre-determined profiles of the atmosphere for dust and water ice derived from daytime data of non-thermally active pixels and apply the derived atmospheric profiles to the anomalous pixel spectra. After accounting for the atmospheric absorptions, silicate activity is again easily spotted at IR wavelengths, with thermal emission at least a hundred times greater than Mars background at 7 μm, dropping to a factor of ~14 at 13 μm (Table 2). With hydrothermal activity, the difference between background and recently frozen water is considerably less than that from silicate activity. The difference is less than a factor of six around 7 μm, but should be detectable if the thermal anomaly is extensive enough.

Thus the lack of detection of a thermal anomaly by THEMIS in the Tharsis/Elysium corridor does not completely eliminate the possibility that this region could still be geothermally active. We can rule out the presence of extensive high-temperature silicate volcanism occurring on the surface today, but low-level hydrothermal activity or episodic silicate volcanism, which is not active at present cannot be ruled out. In addition, the lack of reported thermal anomaly since the acquisition of the THEMIS images may constrain the upper limit of volcanic/hydrothermal activity in this region. The region is unlikely to be as active as most of the Holocene volcanic zones on Earth. Thus, "active" does not necessarily refer to present-day activity, but rather a planetary body that has not reached its cooling threshold, and thus has the potential to release endogenic activity in the future such as in the corridor region. Higher resolution data acquired by other missions, such as MRO will be necessary to further test this hypothesis.

4.2. Geophysical modeling

Early studies of the thermal evolution of Mars were performed using one-dimensional parameterized convection models, which gave solutions for the average temperature as a function of depth (e.g., Spohn, 1991; Schubert et al., 1992). From these models, the general thermal evolution of Mars, from earliest times to most recent, was described by the following steps. The interior of Mars at the end of accretion was very hot, resulting in differentiation within a few hundred Ma. Magmatism and volcanism removed the heat-producing radiogenic elements from the mantle and concentrated them in the crust. This activity caused a significant depletion of heat sources in the mantle, which allowed the mantle to cool more rapidly and increased the lithosphere thickness. A stagnant-lid regime was established early in martian history. The remaining thermal history of Mars has seen a steady decline of mantle temperature and a thickening of the lithosphere to present values (Jackson and Pollack, 1984). Once stagnant-lid convection had been established, all of the heat lost from this system had to be transported by conduction across the rigid lid. Thus, volcanism is not assumed to occur in the later stage of the martian history based on this premise. However, this contradicts the geologic and martian meteorite evidence cited above, which indicates volcanic activity within the last 100–200 Ma (Nyquist et al., 2001; Neukum et al., 2004).

Parameterized convection models, which are used in most thermal evolution studies, calculate one-dimensional temperatures as a function of depth. Volcanic events are usually expressed by arbitrary assumptions about the melt efficiency. Although this approach is appropriate to investigate the long-term overall melt productivity, it is likely oversimplified with regards to volcanic activity. Tharsis, for example, has been modeled as a region of volcanically thickened crust (Solomon and Head, 1982), but a hot underlying mantle would also contribute to the observed topographic uplift. Recent thermal models have assumed a stagnant-lid regime for Mars with localized volcanism resulting from mantle plume activity. Plumes have warmer temperatures than the average mantle, and

therefore can result in local decompression melting and lithospheric thinning above the upwelling convective flow even in the recent history of Mars (Kiefer, 2003). Furthermore, the mantle-derived magma supply for shield volcanoes should be episodic rather than continuous (Mitchell and Wilson, 2003), consistent with mantle models (Schott et al., 2001) and with the evolutional history of Tharsis, which shows evidence of an episodic magmatic complex/superplume (Dohm et al., 2001a, 2007a). Thus, the thermal evolution of the Tharsis/Elysium corridor is more complicated than suggested by simple static cooling via conduction across the stagnant lid.

Recent thermal evolutionary models of Mars highlight three additional points: (1) the importance of estimating the concentrations of the primary heat-producing elements of potassium (K), uranium (U), and thorium (Th), which vary considerably between models (McLennan, 2001; Hauck and Phillips, 2002); (2) the amount of melt production, which is potentially significant for crustal evolution, in terms of partial melting of the mantle caused by decompression of mantle material within convective upwellings (Hauck and Phillips, 2002); and (3) the differentiation of heat-producing elements into the crust (McLennan, 2001; Hauck and Phillips, 2002). Schott et al. (2001) performed two-dimensional numerical simulations of thermochemical evolutions of Mars and showed that sublithospheric hot spots could survive over time scales of several hundred Ma. These hot spots trigger future hot upwellings, which could partly explain the persistent episodic and focused volcanism in the Tharsis region. Kiefer's (2003) model, by changing the total radioactive heating rate and partitioning of radioactive elements between the mantle and crust, was able to generate at least some mantle melting in the present epoch. These numerical simulations suggest that if the martian mantle has retained $50\% \pm 10\%$ of the bulk planet radioactive abundance inferred by Wänke and Dreibus (1994), Mars could still be volcanically active at present. This degree of partitioning of radioactivity between the mantle and crust is geochemically plausible, considering the mean crustal thickness on Mars is estimated to be between 50 and 100 km (Zuber et al., 2000; Nimmo and Stevenson, 2001).

An important consideration in thermal evolutionary models is how much of the planet's bulk K, Th, and U was partitioned into the crust versus remaining in the mantle. Using GRS-elemental concentrations, Taylor et al. (2006) derived an average Th concentration of 0.6 ppm. The thickness of the crust is estimated on geophysical grounds to be somewhere between 29 and 115 km, with a reasonable range of 33–81 km and a nominal value of 57 km (Wieczorek and Zuber, 2004). Assuming a bulk Th concentration throughout Mars of 0.056 ppm (Wänke and Dreibus, 1994), Taylor et al. (2006) calculate that 50% of the Th and K are in the crust. The consequence of sequestering half of the heat-producing elements into the crust early in martian history is that the rate of crustal production becomes very small after about 4 Ga (Hauck and Phillips, 2002), assuming mantle rheology consistent with the presence of water. However, a small rate of crustal production does not imply that there is no recent magmatism. Kiefer (2003) calculated that there could be present-day volcanic eruptions if 43–50% of the radioactive elements remained in the mantle. Thus, the global GRS data for K and Th, as well as the geologic evidence described previously for the Tharsis/Elysium corridor, are consistent with Mars being internally active.

Amazonian tectonism in the corridor region (e.g., Anderson et al., 2001, 2004; Wyrick et al., 2004; Ferrill et al., 2004; Márquez et al., 2004) suggests that Mars as a whole should be more seismically active than the Moon but less active than the Earth (Solomon et al., 1991). In addition, theoretical calculations suggest that stresses associated with cooling of the martian lithosphere should result in seismicity (Golombek et al., 1992), exceeding the rate of non-impact-produced shallow lunar seismicity (28 events in 8 years) (Nakamura, 1980). The future deployment of seismometers in regions such as the Tharsis/Elysium corridor combined with sample return missions that allow absolute dating of materials from known locations will greatly enhance our understanding of Mars' internal evolution (Stevenson, 2001; Zuber, 2001). Such a seismic network will provide insights not only in determining whether Mars is seismically active, but also can help determine whether magma reservoirs occur at depth in the corridor region.

5. Tharsis/Elysium corridor as a prime site for future exploration

Existing geological, geomorphic, geophysical, topographic, impact cratering, spectral, and elemental information collectively suggest that future exploration in the Tharsis/Corridor region (see Fig. 1) could yield significant geologic (including whether Mars is still active), paleoclimatic, paleohydrologic, and possibly biologic information such has been proposed for the NSVs region (Dohm et al., 2004). In the following, we present a possible terrestrial analog to the Tharsis–Elysium corridor and then discuss the astrobiologic relevance of Mars, and in particular, the Tharsis/Elysium corridor.

5.1. *Solfatara Crater, Italy, as a terrestrial analog*

5.1.1. *Introduction*

Terrestrial analogs are locations on Earth that are believed to bear some resemblance to past or present geologic and environmental conditions hypothesized for another planet. For example, lessons learned from studies in the Channeled Scablands of eastern Washington were successfully used to predict the environment later encountered by Mars Pathfinder in Ares Valles (Golombek et al., 1999). However, we must remember that no terrestrial site can exactly replicate what is likely to be found at its martian analog due to the very complex geologic histories,

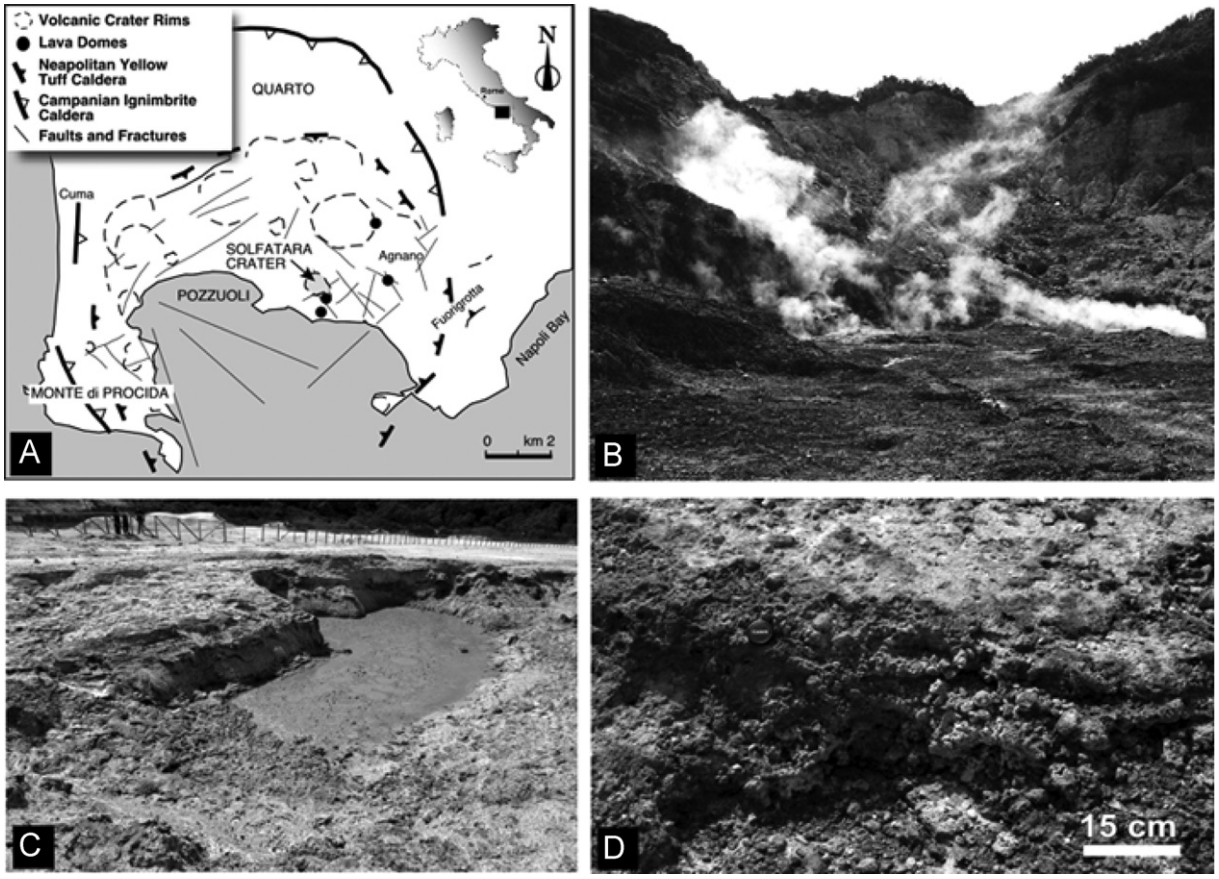

Fig. 13. (A) Sketch map of the Campi Flegrei volcanic area (modified from Di Vito et al., 1999). (B) Fumaroles close to northeastern wall of the Solfatara crater. Also visible are the highly weathered crater floor (foreground) and the pyroclastic material, which forms the wall (background). (C) A hot mud pool with continuous release of bubbling gases in the central pazrt of the Solfatara crater. (D) Hydrothermal mineralized crusts containing iron oxides develop close to the fumarolic active area.

different environments, and histories either obscured or destroyed by erosion or burial. New data also often changes our perspectives of what constitutes a good terrestrial analog site. For example, Yellowstone has been extensively used as an analog to hypothesized hydrothermal systems on Mars, especially because it is considered to be a supervolcano with a caldera more than 100 km across (similar to some of the constructs of Tharsis), which includes basaltic compositions (e.g., Schulze-Makuch et al., 2005a). However, recent spectroscopic data are revealing Mars to be a more geologically diverse planet than has been previously reported, revealing evidence of quartz, sulfates, and clays in addition to basalt (e.g., Rieder et al., 2004; Christensen et al., 2005; Gendrin et al., 2005; Bibring et al., 2006). Thus, we must identify additional terrestrial analog sites that include silicic volcanic centers associated with plume activity. Volcanism occurring along tectonically active regions also should be considered since plate tectonics (Sleep, 1994) cannot be ruled out during ancient Mars (e.g., Baker et al., 2002; Fairén and Dohm, 2004; Márquez et al., 2004; Connerney et al., 2005). Based on a synthesis of the information presented above, we suggest Solfatara Crater as a suitable terrestrial analog representative of the Tharsis–Elysium corridor.

5.1.2. Geological background

Similar to hydrothermal-recording Solfatara Crater, the corridor is expected to record pervasive ancient and possibly extant hydrothermal activity. In addition, though orbital data such as acquired through the MEx Omega and MGS TES instruments are showing mostly spectral signatures interpreted to be dust as described in Section 3.3, the presented diverse information underscores the need for acquiring HiRISE and CRISM data and continued investigation. Therefore, though the potential diversity of rock types may be obscured by fine-grained materials such as dust or possibly aqueous alteration, or both, we deem the Solfatara Crater to be an appropriate analog, providing significant compositional information that may be encountered in the corridor region.

Solfatara Crater is a flat-bottomed volcanic crater with steep-sided walls 80–85 m high, located in southern Italy (Fig. 13A). The caldera is elliptical with a major axis of 770 m and a minor axis of 580 m. Solfatara crater is part of the Campi Flegrei volcanic district, represented by a nested 12-km-wide structure of calderas and small volcanic edifices (Fig. 13A). Campi Flegrei has been active during the Quaternary (at least since 47,000 years ago) and is linked to the extensional tectonics of the Tyrrhenian margin. This district is connected with the Somma–Vesuvio

volcanic complex to the southwest, but there is no interdependency on the volcanic activity of these two provinces. Campi Flegrei has been characterized by two major eruptive sequences, the Campanian Ignimbrite (~37,000 ago) and the Neapolitan Yellow Tuff (~12,000 years ago), which led to two main caldera collapses (Fig. 13A). The composition of the eruptive products ranges from trachyte to latite (Orsi et al., 1996) with a marked phreatomagmatic characteristic for the Neapolitan Yellow Tuff (Wohletz et al., 1995). The variations in eruptive dynamics within the Campi Flegrei district are caused by the magma flowing underground from one caldera to another. This mechanism is also responsible for a still active bradisism process, which causes the slow inflation and deflation of the surface.

The volcanic activity of Solfatara started about 4000 years ago. The volcanic history is characterized by both explosive and effusive eruptions, which occurred within short-time intervals, similar to the episodic activity proposed for the Tharsis/Elysium corridor. Pyroclastic deposits are trachytic in composition, whereas older lava domes are made of K-phonolites (Rosi and Sbrana, 1987).

Solfatara shows continuous fumarolic activity (Fig. 13B) on the northeastern side and emissions of sputtering mud (Fig. 13C) in the central sector of the crater. This latter activity forms several mud pools, a few meters wide and 1–2 m deep (Fig. 13C). The depth of water in the pools is basically controlled by the groundwater table. During the rainy season, the water may rise to overbanking stage, flooding a large portion of the crater floor. The hydrothermal system is vapor dominated and fed by a 1.5-km deep, low-permeability, geothermal aquifer of mixed magmatic–meteoric origin (Chioni et al., 1984). The fluids record temperatures ranging from ~160 °C for the hottest fumarole to 40–50 °C for areas around the major emission points and pH of approximately 1.7.

The shape and activity of Solfatara crater is strongly controlled by NE-trending fractures. Both fumaroles and mud pools are linked to this fracture system, but some of the features connected to the mud pools are apparently more active. Between 1982 and 1984, fracture movements occurred in association with a slow uplift of the crater floor (in excess of 2 m). During this event, many mud pools that existed in the central part of the crater were totally drained.

5.1.3. Hydrothermal activity and related alteration

Hydrothermal fluids migrating through the deposits are rich in H_2S, CO_2 and, secondarily, HCl, CH_4, and H_2, (Valentino et al., 1999), producing chemical conditions which are predominantly anoxic and reducing. Oxic/anoxic transition zones exist on limited surface areas and within rock fractures. The hydrothermal deposits of Solfatara (Fig. 13D) include sulfur, sulfates (gypsum, barite), hydrous sulfates (alunite), and pyrite. Minor occurrences of likely abiotic magnetite have been observed in the mineralized crusts (Rosi and Sbrana, 1987; Glamoclija et al., 2004).

Sulfur is one of the major chemical components that have been detected in martian surface materials. Viking and Pathfinder chemical analysis revealed SO_3 concentrations for soil and dust in the range of 4–7 wt% (Clark et al., 1982; Wänke et al., 2001). MEx's OMEGA instrument has recently detected the presence of various sulfate phases on the martian surface, including gypsum, alunite, kieserite, and Mg/Ca sulfates (Clark et al., 1982, 2005; Banin et al., 1997; Bishop et al., 2002; Gendrin et al., 2005; Langevin et al., 2005). The Mars Exploration Rovers have detected at least 30–40 wt% of magnesium sulfates at both Endurance Crater (Meridiani Planum) and Husband Hill (Columbia Hills, in Gusev Crater) (Squyres et al., 2004). A variety of Fe-bearing sulfates (jarosite, natrojarosite) have been suggested to form as possible phases under oxidative, acidic weathering conditions at the surface of Mars (Burns and Fisher, 1990; Bell, 1996), possibly inhibiting the formation of carbonates at the surface (Fairén et al., 2004), and have been observed in the outcrops in Meridiani Planum (Klingelhöfer et al., 2004). Additionally, small amounts of Ca and Mg sulfates and sulfides (pyrrhotite, pyrite) have been identified in the SNC meteorites (McSween, 1994).

Multiple alteration processes such as palagonitic, pedogenic, or solfataric related to volcanic tephra, ash, or lava have been used to model martian surface processes forming sulfates and iron mineral phases (Bell et al., 1993; Banin et al., 1997; Tosca et al., 2004; Hurowitz et al., 2006; Chevrier and Mathé, 2007). Laboratory simulations indicate that the sulfates and (oxy)hydroxides observed on the surface of Mars can form through weathering processes in conditions similar to present-day and past martian conditions, as well as in the Solfatara Crater (Bishop et al., 2002; Golden et al., 2004; Chevrier et al., 2004, 2006). Hydrothermal alteration and meteoritic weathering of Solfatara tephra results in the formation of sulfate (gypsum, alunite), sulfide (pyrite), and iron oxy/hydroxide mineral phases, and thus making the Solfatara Crater a relevant analog of the volcanic regions of Mars, and in particular, the Tharsis/Elysium corridor.

One of the regions reported to exhibit enhanced concentrations of atmospheric methane is the Tharsis/Elysium corridor (Krasnopolshy et al., 2004; Formisano et al., 2004). These small amounts of CH_4 are significant since they may be derived from recent volcanism, hydrothermal/hydrologic activity, and/or biologic release. The residence time for CH_4 in the martian atmosphere is on the order of 10^2 years, indicating that the methane must be constantly replenished (e.g., Formisano et al., 2004). The emission of methane from Solfatara Crater enhances its appropriateness as a terrestrial analog for the Tharsis/Elysium corridor.

5.1.4. Biology and astrobiology relevance

Chemical reactions of hydrothermal weathering, which dominate Solfatara's environment, have been proposed as one of the possible pathways for martian surface alteration

processes. Acidic, hot environments of mud pools and fumaroles such as seen at Solfatara are examples of extreme terrestrial environments that are inhabited by thermoacidophilic and chemosynthetic microbial communities (Glamoclija et al., 2004). The habitat characteristics control the development of different types of microbial–metabolic pathways, in accordance with the available chemical compounds. Reduced constituents derived from hydrothermal fluids are generally far from equilibrium with their oxidized counterparts, making possible the coexistence of sulfide oxidizers and sulfur disproportionating bacteria to iron-oxidizing and methanotrophic life forms. Mineral biosignatures have been identified in the mineralized crusts of Solfatara and are mostly related to elemental sulfur (S^0), pyrite (Fe_2S), and barite ($BaSO_4$) crystals, which were in some cases associated with iron oxy/hydroxide permineralized extracellular polymers (EPS) structures (Glamoclija et al., 2004). Though the precipitation of Ba and SO_4 is clearly an abiotic reaction, bacteria sulfide oxidizers or sulfur disproportionating bacteria may have contributed to an increase in the local SO_4 concentration. Iron oxy/hydroxide (goethite-like) mineralization has also been identified and interpreted as related to bacterial activity (Glamoclija et al., 2004). At Solfatara, alunite ($KAl_3(SO_4)_2(OH)_6$) crystals from the jarosite mineral group have been suggested as a probable inorganic biosignature. Although alunite is abiotically formed, sulfide oxidizers might contribute to increase local H_2SO_4, thus triggering the formation of this mineral (Glamoclija et al., 2004).

Solfatara Crater clearly displays the interaction between magmatic, tectonic, and fluvial activity, which is also suggested in the Tharsis/Elysium corridor. Furthermore, Solfatara genomes, their physiology, and preferential ways of permineralization during the fossilization process and related biosignatures represent a contemporary model system, which may help in interpreting ancient putative biogenic traces on Earth and, eventually, their possible martian counterparts. We therefore consider it to be a prime ground-truthing site for mission design, development, and testing that will lead to optimal remote reconnaissance of the Tharsis/Elysium corridor. The significant geologic, hydrologic, geochemical, geophysical, and biological information which results from detailed studies of Solfatara will provide important insights into what we could potentially encounter in the Tharsis/Elysium corridor.

5.2. *Life potential on Mars through the Tharsis/Elysium corridor*

The availability of water throughout martian history and its possible presence up to the present time point to Mars as a prime target for astrobiological investigations. The previous discussion strongly suggests a planet that has been internally active at least until geologically recent time, well into the Late Amazonian. These conditions of liquid water and energy sources, as particularly highlighted in the Tharsis/Elysium corridor, make it reasonable to infer that life could have originated independently on Mars, especially since extremely ancient environmental conditions were likely very similar to those on Earth 4.5 to 4.0 Gyr ago (Fairén and Dohm, 2004). These conditions include inferred ancient long-term liquid water stability on the surface, a thick atmosphere, a magnetic field, plate tectonism, and elevated geothermal activity (Baker et al., 2002, 2007; Watson and Harrison, 2005). Alternatively, life might have been transferred to Mars by impact panspermia from Earth (Melosh, 1988; Davies, 1996). However, impact transpermia from Mars to Earth would be more likely due to the Sun's gravity sink in the center of the solar system (Schulze-Makuch et al., 2005a).

Once life gained a foothold on Mars, it would adapt to the planet's changing climatic conditions. In a constant environment, evolutionary options narrow to stable forms that persist with little change through time (stabilizing selection), while in a changing environment, evolution favors selection of new forms and function (directional selection, Schulze-Makuch and Irwin, 2004). Mars appears to have been cold and dry for most of its history, but has been subject to periodic global flooding triggered by episodic volcanism and meteorite bombardment, and localized flow from snowmelt or groundwater eruptions (Carr, 1990; Malin and Edgett, 2000; Berman and Hartmann, 2002; Segura et al., 2002; Christensen et al., 2003). These conditions suggest that the first life forms could have been either chemoautotrophs or heterotrophs and that phototrophic microbes could have originated as well. The rapidly changing conditions suggest a strong directional selection for enhancing chemoautotrophy and the development of alternative energy sources. Strong directional selection for life cycles alternating between dormant and proliferative forms would likely have occurred (Schulze-Makuch et al., 2005a, b). The conditions would be conducive to the transferal of life from the subsurface to the surface, especially during magmatic-induced flooding and associated water bodies ranging from oceans to lakes (Dohm et al., 2001a, b; Fairén et al., 2003) and transient climate change (Baker et al., 1991). The persistence of some chemotrophs and organisms that might use alternative energy sources (such as thermal energy; Schulze-Makuch and Irwin, 2002) below the surface would be possible at the present time. This would lead to microscopic life forms existing in subterranean environments including groundwater aquifers or caves with putative hydrothermal sites.

The small amounts of methane detected in the martian atmosphere could be biologically produced (Krasnopolshy et al., 2004). The CH_4 could be derived from the destabilization of methane hydrates formed by chemoautotrophic bacterial communities on a Noachian seafloor, from a contemporary deep biosphere of methanogens in martian groundwater isolated below the ice-rich permafrost (Chapelle et al., 2002; Chastain and Chevrier, 2007),

or from inorganic processes including hydrothermal activity and clathrate destabilization (Prieto-Ballesteros et al., 2006). Martian life may have evolved alternating cycles between active and dormant forms, in which case microbes could be present in dormant forms close to the surface and in active forms in protected environments. Periodic liquid water on Mars could have provided opportunities for biologic activity (Cabrol et al., 2001; Fairén et al., 2005), as well as evolutionary progress. This would be especially true at the surface during the hypothesized Tharsis-induced flooding episodes and associated ponding, resulting in transient climatic perturbations (Baker et al., 1991; Dohm et al., 2001a; Fairén et al., 2003; Schulze-Makuch et al., 2005a, b). In this case, organic macromolecules, fossil fragments, and possibly dormant microbial forms could be found close to the martian surface, as in the possible case of the Tharsis/Elysium corridor region.

6. Conclusions

We have presented a synthesis of the geologic and compositional evidence indicating that the Tharsis/Elysium corridor records a long-lived history of magmatic–tectonic-water interactions which have continued into recent times and may still be active today. The once persistent paradigm of a mostly basaltic, early warm and wet Mars that later became a geologically dead and dry desert planet is being transformed by new mission data. First, the idea of a cold dry planet has required re-examination as a result of recent OMEGA mineralogical results suggest that the global martian environment has transitioned from a water-rich planet early in its history through a period of highly acidic conditions to the current relatively dry environment (Bibring et al., 2006), although localized regions of more recent aqueous activity cannot be ruled out. MGS, MO, and MER have discovered evidence of localized water-enriched regions occurring throughout martian history (Malin and Edgett, 2000; Squyres et al., 2004). GRS findings show that the polar regions and selected equatorial areas display elevated H signatures that may signify hydrated minerals, water/water ice, interstitial brine solutions, −OH radicals, or a combination of these (Boynton et al., 2002; Feldman et al., 2002). The new data reveal evidence of geologically recent climatic change (e.g., Scott and Zimbelman, 1995; Scott et al., 1998; Head et al., 2003a; Márquez, et al., 2004), consistent with geologic and paleohydrologic information. Second, the idea of a mostly basaltic Mars is also being transformed due to the MGS, MO, MEx, and MER data, which are showing a more geologically diverse planet with exposures of hematite, quartz, andesite, sulfates, and layered sedimentary deposits, etc. (e.g., Malin and Edgett, 2000; Bandfield et al., 2000, 2004; Christensen et al., 2000, 2001a, b, 2005; Rieder et al., 2004; Gendrin et al., 2005; Bibring et al., 2006).

Finally, the idea that Mars is geologically dead at the present time is called into question by various lines of evidence that have been revealed in the Tharsis/Elysium corridor, including geologic, geomorphic, paleohydrologic, paleotectonic, and elemental expressions of the martian surface.

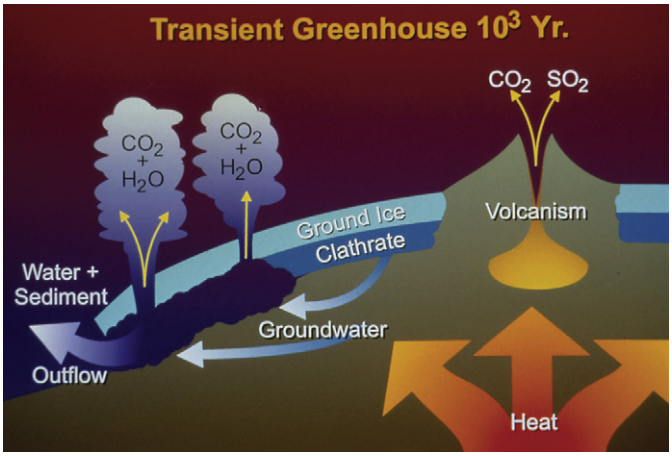

Fig. 14. Schematic diagram showing the Mars Episodic Glacial Atmospheric Oceanic Upwelling by Thermotectonic FLood Outbursts (MEGA-OUTFLO) hypothesis of Baker et al. (1991, 2000). This genetic model ascribes the episodic formation of Oceanus Borealis to cataclysmic outburst flooding of the outflow channels. Baker et al. (2000) suggests a mechanism whereby CO_2 clathrate in the martian permafrost zone is destabilized by episodes of very high heat flow, such that released CO_2 from the lower permafrost zone (2–3 km depth) and dissolved CO_2 from the underlying groundwater explosively forces out pressurized slurries of water and fractured rock fragments in massive outbursts. The huge floods form Oceanus Borealis as the atmosphere is being transformed by released CO_2 to a transient greenhouse condition. Subsequent sediment-charged water enters the ocean as hyperpycnal flows, generating density flows that extend deposits across the northern plains. This hypothesis explains the long epochs ($\sim 10^8+$ years), during which the Mars surface had extremely cold, dry conditions similar to those prevailing today, terminated by short-duration ($\sim 10^4$–10^5 years) episodes of much warmer, wetter conditions associated with a transient greenhouse climate.

An internally active Mars has tremendous implications, including: (1) a potential for continuing magmatic-driven activity, including volcanism, tectonism, hydrothermal activity, and related climatic response (Fig. 14); (2) regions of elevated heat flow that may interact with near-surface groundwater to produce active hydrothermal systems; and (3) possible near-surface life. We suggest that further investigations of terrestrial analogs such as Solfatara Crater, Italy, will help us better prepare to unfold the exciting possibilities that await discovery by future science-driven robotic (through designs such as proposed by Fink et al. (2005)) and piloted missions in the Tharsis/Elysium corridor.

Acknowledgments

We are grateful to Goro Komatsu, Vincent F. Chevrier, and anonymous reviewer for their thoughtful reviews, all of which resulted in a significantly improved manuscript. We are also grateful to the Gamma Ray Spectrometer Team whose diligent efforts have yielded tremendous fruit.

References

Abe, Y., Numaguti, A., Komatsu, G., Kobayashi, Y., 2005. Four climate regimes on a land planet with wet surface: effects of obliquity change and implications for ancient Mars. Icarus 178, 27–39.

Anderson, R.C., Dohm, J.M., Golombek, M.P., Haldemann, A., Franklin, B.J., Tanaka, K.L., Lias, J., Peer, B., 2001. Significant centers of tectonic activity through time for the western hemisphere of Mars. J. Geophys. Res. 106, 20,563–20,585.

Anderson, R.C., Dohm, J.M., Haldemann, A.F.C., Hare, T.M., Baker, V.R., 2004. Tectonic histories between Alba Patera and Syria Planum, Mars. Icarus 171, 31–38.

Anderson, R.C., Dohm, J.M., Golombek, M., Haldemann, A.F.C., Pounders, E., 2007a. Centers of tectonism identified for the western and eastern hemisphere of Mars. Lunar Planet. Sci. Conf. XXXVIII #1889 (abstract) (CD-ROM).

Anderson, R.C., Dohm, J.M., Haldemann, A.F.C., Pounders, E., Golombek, M., Castano, A., 2007b. Centers of tectonic activity for the eastern hemisphere of Mars. Icarus, in press.

Baker, V.R., 2001. Water and the martian landscape. Nature 412, 228–236.

Baker, V.R., Strom, R.G., Gulick, V.C., Kargel, J.S., Komatsu, G., Kale, V.S., 1991. Ancient oceans, ice sheets and the hydrological cycle on Mars. Nature 352, 589–594.

Baker, V.R., Strom, R.G., Dohm, J.M., Gulick, V.C., Kargel, J.S., Komatsu, G., Ori, G.G., Rice Jr., J.W., 2000. Mars' Oceanus Borealis, ancient glaciers, and the MEGAOUTFLO hypothesis. Lunar Planet. Sci. Conf. (CD-ROM) XXXI abstract 1863.

Baker, V.R., Maruyama, S., Dohm, J.M., 2002. A theory of early plate tectonics and subsequent long-term superplume activity on Mars. Superplume International Workshop, Abstracts with Programs, Tokyo, pp. 312–316.

Baker, V.R., Maruyama, S., Dohm, J.M., 2007. Tharsis superplume and the geological evolution of early Mars. In: Yuen, D.A., Maruyama, S., Karato, S.-I., Windley, B.F. (Eds.), Superplumes: Beyond Plate Tectonics. Springer, Berlin, pp. 507–523.

Bandfield, J.L., Hamilton, V.E., Christensen, P.R., 2000. A global view of martian surface compositions from MGS-TES. Science 287, 1626–1630.

Bandfield, J.L., Hamilton, V.E., Christensen, P.R., McSween Jr., H.Y., 2004. Identification of quartzofeldspathic materials on Mars. J. Geophys. Res. 109 (E10009).

Banerdt, W.B., Golombek, M.P., Tanaka, K.L., 1992. Stress and tectonics on Mars. In: Kieffer, H.H., Jakosky, B.M. (Eds.), Mars. University of Arizona Press, pp. 249–297.

Banin, A., Han, F.X., Cicelsky, A., 1997. Acidic volatiles and the Mars soil. J. Geophys. Res. 102, 13.341–13.356.

Barlow, N.G., 1988. Crater size-frequency distributions and a revised martian relative chronology. Icarus 75, 285–305.

Barlow, N.G., 2006. The production rate and distribution of secondary craters on Mars. Workshop on Surface Ages and Histories: Issues in Planetary Chronology. LPI Contribution #1320, pp. 12–13.

Bell III, J.F., 1996. Iron, sulfate, carbonate, and hydrated mineral on Mars. In: Dyar, M.D., McCammon, C., Schaefer, M.W. (Eds.), Mineral Spectroscopy: A Tribute to Roger G. Burns. Geochem. Soc. Special Pub. No. 5, pp. 359–380.

Bell III, J.F., Morris, R.V., Adams, J.B., 1993. Thermally altered palagonitic tephra: a spectral and process analog to the soil and dust of Mars. J. Geophys. Res 98, 3373–3385.

Berman, D.C., Hartmann, W.K., 2002. Recent fluvial, volcanic, and tectonic activity on the Cerberus plains of Mars. Icarus 159 (1), 1–17.

Bibring, J.-P., Langevin, Y., Mustard, J.F., Poulet, F., Arvidson, R., Gendrin, A., Gondet, B., Mangold, N., Pinet, P., Forget, F., OMEGA team, 2006. Global mineralogical and aqueous Mars history derived from OMEGA/Mars Express data. Science 312, 400–404.

Bishop, J.L., Murchie, S.L., Pieters, C.M., Zent, A.P., 2002. A model for formation of dust, soil, and rocks coatings on Mars: physical and chemical processes on the martian surface. J. Geophys. Res. 107, 5097/17.

Borg, L.E., Nyquist, L.E., Weissman, H., Shih, C.Y., Reese, Y., 2003. The age of Dar al Gani 476 and the differentiation history of the martian meteorites inferred from their radiogenic isotopic systematics. Geochim. Cosmochim. Acta 67, 3519–3536.

Boynton, W.V., Feldman, W.C., Squyres, S.W., Prettyman, T.H., Brückner, J., Evans, L.G., Reedy, R.C., Starr, R., Arnold, J.R., Drake, D.M., Englert, P.A.J., Metzger, A.E., Mitrofanov, I., Trombka, J.I., d'Uston, C., Wänke, H., Gasnault, O., Hamara, D.K., Janes, D.M., Marcialis, R.L., Maurice, S., Mikheeva, I., Taylor, G.J., Tokar, R., Shinohara, C., 2002. Distribution of hydrogen in the near surface of Mars: evidence for subsurface ice deposits. Science 297, 81–85.

Boynton, W.V., Feldman, W.C., Mitrofanov, I.G., Evans, L.G., Reedy, R.C., Squyres, S.W., Starr, R., Trombka, J.I., d'Uston, C., Arnold, J.R., Englert, P.A.J., Metzger, A.E., Wänke, H., Brückner, J., Drake, D.M., Shinohara, C., Fellows, C., Hamara, D.K., Harshman, K., Kerry, K., Turner, C., Ward, M., Barthe, H., Fuller, K.R., Storms, S.A., Thornton, G.W., Longmire, J.L., Litvak, M.L., Ton' Chev, A.K., 2004. The Mars Odyssey Gamma-Ray Spectrometer Instrument Suite. Space Sci. Rev. 110, 37–83.

Boynton, W.V., et al., 2007. Concentration of H, Si, Cl, K, Fe, and Th in the low- and mid-latitude regions of Mars. J. Geophys. Res. 112, E12S99, doi:10.1029/2007JE002887.

Brandon, A.D., Walker, R., Morgan, J.W., Goles, G.G., 2000. Re–Os isotopic evidence for early differentiation of the martian mantle. Geochim. Cosmochim. Acta 64, 4083–4095.

Breuer, D., Spohn, T., 2003. Early plate tectonics versus single-plate tectonics on Mars: evidence from magnetic field history and crust evolution. J. Geophys. Res. 108, 5072.

Bridges, J., Catling, D.C., Saxton, J.M., Swindle, T.D., Lyon, I.C., Grady, M.M., 2001. Alteration assemblages in martian meteorites: implications for near-surface processes. Space Sci. Rev. 96, 365–392.

Burns, R.G., Fisher, D.S., 1990. Iron-sulfur mineralogy of Mars: magmatic evolution and chemical weathering products. J. Geophys. Res. 95, 14415–14421.

Burr, D.M., Grier, J.A., McEwen, A.S., Keszthelyi, L.P., 2002. Repeated aqueous flooding from the Cerberus Fossae: evidence for very recently extant, deep groundwater on Mars. Icarus 159, 53–73.

Cabrol, N.A., Grin, E.A., Landheim, R., Kuzmin, R.O., Greeley, R., 1998. Duration of the Ma'adim Vallis/Gusev crater hydrogeologic system, Mars. Icarus 133, 98–108.

Cabrol, N.A., Wynn-Williams, D.D., Crawford, D.A., Grin, E.A., 2001. Recent aqueous environments in martian impact craters: an astrobiological perspective. Icarus 154, 98–113.

Carr, M.H., 1990. D/H on Mars: the effect of floods, volcanism, impacts and polar processes. Icarus 87, 210–227.

Carr, M.H., 1996. Water on Mars. Oxford University Press, New York, 229pp.

Carr, M.H., Chuang, F.C., 1997. Martian drainage densities. J. Geophys. Res. 102, 9145–9152.

Chapelle, F.H., O'Neill, K., Bradley, P.M., Meth, B.A., Ciufo, S.A., Knobel, L.L., Lovley, D.R., 2002. A hydrogen-based subsurface microbial community dominated by methanogens. Nature 415, 312–315.

Chapman, M.G., Tanaka, K.L., 1993. Geologic map of the MTM-05152 and -10152 quadrangles, Mangala Valles region of Mars. USGS Misc. Inv. Ser. Map I-2294 (1:500,000).

Chapman, M.G., Tanaka, K.L., 1996. Geologic maps of the MTM 25062 quadrangle (digital compilation) and the MTM 25067 quadrangle (manual compilation), Kasei Valles region of Mars. USGS Misc. Inv. Ser. Map I-2398 (1:500,000).

Chapman, M.G., Masursky, H., Scott, D.H., 1991. Geologic map of science study area 2, north Kasei Valles, Mars (MTM 25072 quadrangle). USGS Misc. Inv. Ser. Map I-2107 (1:500,000).

Chastain, B.K., Chevrier, V., 2007. Methane clathrate hydrates as a potential source for martian atmospheric methane. Planet. Space Sci. 55, 1246–1256.

Chevrier, V., Mathé, P.E., 2007. Mineralogy and evolution of the surface of Mars: a review. Planet. Space Sci. 55, 289–314.

Chevrier, V., Rochette, P., Mathé, P.-E., Grauby, O., 2004. Weathering of iron rich phases in simulated martian atmospheres. Geology 32, 1033–1036.

Chevrier, V., Mathe, P.E., Rochette, P., Grauby, O., Bourrie, G., Trolard, F., 2006. Iron weathering products in a $CO_2+(H_2O$ or $H_2O_2)$ atmosphere: implications for weathering processes on the surface of Mars. Geochim. Cosmochim. Acta 70, 4295–4317.

Chioni, R., Corazza, E., Marini, L., 1984. The gas/steam ratio as indicator of heat transfer at the Solfatara fumarole, Phlegrean Fields (Italy). Bull. Volcanol. 47, 295–302.

Christensen, P.R., Bandfield, J.L., Smith, M.D., Hamilton, V.E., Clark, R.N., 2000. Identification of a basaltic component on the martian surface from Thermal Emission Spectrometer data. J. Geophys. Res. 105, 9609–9621.

Christensen, P.R., Bandfield, J.L., Hamilton, V.E., Ruff, S.W., Kieffer, H.H., Titus, T.N., Malin, M.C., Morris, R.V., Lane, M.D., Clark, R.L., Jakosky, B.M., Mellon, M.T., Pearl, J.C., Conrath, B.J., Smith, M.D., Clancy, R.T., Kuzmin, R.O., Roush, T., Mehall, G.L., Gorelick, N., Bender, K., Murray, K., Dason, S., Greene, E., Silverman, S., Greenfield, M., 2001a. The Mars Global Surveyor Thermal Emission Spectrometer experiment: investigation description and surface science results. J. Geophys. Res. 106, 23,823–23,871.

Christensen, P.R., Morris, R.V., Lane, M.D., Bandfield, J.L., Malin, M.C., 2001b. Global mapping of martian hematite mineral deposits: remnants of water-driven processes on early Mars. J. Geophys. Res. 106, 23,873–23,886.

Christensen, P.R., Bandfield, J.L., Bell III, J.F., Gorelick, N., Hamilton, V.E., Ivanov, A., Jakosky, B.M., Kieffer, H.H., Lane, M.D., Malin, M.C., McConnochie, T., McEwen, A.S., McSween Jr., H.Y., Mehall, G.L., Moersch, J.E., Nealson, K.H., Rice Jr., J.W., Richardson, M.I., Ruff, S.W., Smith, M.D., Titus, T.N., Wyatt, M.B., 2003. Morphology and composition of the surface of Mars: Mars Odyssey THEMIS results. Science 300, 2056–2061.

Christensen, P.R., Jakosky, B.M., Kieffer, H.H., Malin, M.C., McSewwn, H.Y., Nealson, K., Mehall, G.L., Silverman, S.H., Ferry, S., Caplinger, M., Ravine, M., 2004. The Thermal Emission Imaging System (THEMIS) for the Mars 2001 Odyssey Mission. Space Sci. Rev. 110, 85–130.

Christensen, P.R., McSween Jr., H.Y., Bandfield, J.L., Ruff, S.W., Rogers, A.D., Hamilton, V.E., Gorelick, N., Wyatt, M.B., Jakosky, B.M., Kieffer, H.H., Malin, M.C., Moersch, J.E., 2005. Evidence for magmatic evolution and diversity on Mars from infrared observations. Nature 436, 504–509.

Clifford, S.M., Parker, T.J., 2001. The evolution of the martian hydrosphere: implications for the fate of a primordial ocean and the current state of the northern plains. Icarus 154, 40–79.

Clark, B.C., Baird, A.K., Weldon, R.J., Tsusaki, D.M., Schnabel, L., Candelaria, M.P., 1982. Chemical composition of martian fines. J. Geophys. Res. 87, 10059–10067.

Clark, B.C., Morris, R.V., McLennan, S.M., Gellert, R., Jolliff, B., Knoll, A.H., Squyres, S.W., Lowenstein, T.K., Ming, D.W., Tosca, N.J., Yen, A., Christensen, P.R., Gorevan, S., Brückner, J., Calvin, W., Dreibus, G., Farrand, W., Klingelhoefer, G., Waenke, H., Zipfel, J., Bell III, J.F., Grotzinger, J., McSween Jr., H.Y., Rieder, R., 2005. Chemistry and mineralogy of outcrops at Meridiani Planum. Earth Planet. Sci. Lett. 240, 73–94.

Connerney, J.E.P., Acuña, M.H., Ness, N.F., Kletetschka, G., Mitchell, D.L., Lin, R.P., Reme, H., 2005. Tectonic implications of Mars crustal magnetism. Science 102, 14970–14975.

Craddock, R.A., Greeley, R., 1994. Geologic map of the MTM -20147 quadrangle, Mangala Valles region of Mars. USGS Misc. Inv. Ser. Map I-2310 (1:500,000).

Davies, P.C.W., 1996. The transfer of viable microorganisms between planets. In: Bock, G.R., Goode, J.A. (Eds.), Evolution of Hydrothermal Ecosystems on Earth (and Mars?). Ciba Foundation Symposium 202. Wiley, Chichester, pp. 304–317.

DeHon, R.A., 1992. Geologic map of the Pompeii quadrangle (MTM 20057), Maja Valles region of Mars. USGS Misc. Inv. Ser. Map I-2203 (1:500,000).

DeHon, R.A., Mouginis-Mark, P.J., Brick, E.E., 1999. Geologic map of the Galaxias quadrangle (MTM 35217) of Mars. USGS Misc. Inv. Ser. Map I-2579 (1:500,000).

Di Vito, M.A., Isaia, R., Orsi, G., Southon, J., de Vita, S., D'Antonio, M., Pappalardo, L., Piochi, M., 1999. Volcanism and deformation in the past 12 ka at the Campi Flegrei caldera (Italy). J. Volacanol. Geotherm. Res. 91, 221–246.

Dohm, J.M., Tanaka, K.L., 1999. Geology of the Thaumasia region, Mars: plateau development, valley origins, and magmatic evolution. Planet. Space Sci. 47, 411–431.

Dohm, J.M., Anderson, R.C., Tanaka, K.L., 1998. Digital structural mapping of Mars. Astron. Geophys. 39 (3), 3.20–3.22.

Dohm, J.M., Ferris, J.C., Baker, V.R., Anderson, R.C., Hare, T.M., Strom, R.G., Barlow, N.G., Tanaka, K.L., Klemaszewski, J.E., Scott, D.H., 2001a. Ancient drainage basin of the Tharsis region, Mars: potential source for outflow channel systems and putative oceans or paleolakes. J. Geophys. Res. 106, 32,943–32,958.

Dohm, J.M., Anderson, R.C., Baker, V.R., Ferris, J.C., Rudd, L.P., Hare, T.M., Rice Jr., J.W., Casavant, R.R., Strom, R.G., Zimbelman, J.R., Scott, D.H., 2001b. Latent activity for western Tharsis, Mars: significant flood record exposed. J. Geophys. Res. 106, 12,301–12,314.

Dohm, J.M., Tanaka, K.L., Hare, T.M., 2001c. Geologic map of the Thaumasia region of Mars. US Geol. Survey Map I-2650.

Dohm, J.M., Maruyama, S., Baker, V.R., Anderson, R.C., Ferris, J.C., Hare, T.M., 2002a. Plate tectonism on early Mars: diverse geological and geophysical evidence. Lunar Planet. Sci. Conf. XXXIII #1639 (abstract) (CD-ROM).

Dohm, J.M., Maruyama, S., Baker, V.R., Anderson, R.C., Ferris, J.C., Hare, T.M., 2002b. Evolution and traits of Tharsis superplume, Mars. Superplume International Workshop, Abstracts with Programs, Tokyo, pp. 406–410.

Dohm, J.M., Ferris, J.C., Barlow, N.G., Baker, V.R., Mahaney, W.C., Anderson, R.C., Hare, T.M., 2004. The Northwestern Slope Valleys (NSVs) region, Mars: a prime candidate site for the future exploration of Mars. Planet. Space Sci. 52, 189–198.

Dohm, J.M., Baker, V.R., Maruyama, S., Anderson, R.C., 2007a. Traits and evolution of the Tharsis superplume, Mars. Yuen, D.A., Maruyama, S., Karato, S.-I., Windley, B.F., (Eds.), Springer, Berlin, pp. 523–537.

Dohm, J.M., Barlow, N.G., Anderson, R.C., Williams, J.-P., Miyamoto, H., Ferris, J.C., Strom, R.G., Taylor, G.J., Fairén, A.G., Baker, V.R., Boynton, W.V., Keller, J.M., Kerry, K., Janes, D., Rodríguez, A., Hare, T.M., 2007b. Possible ancient giant basin and related water enrichment in the Arabia Terra province, Mars. Icarus, doi:10.1016/j.icarus.2007.03.006.

Fairén, A.G., Dohm, J.M., 2004. Age and origin of the lowlands of Mars. Icarus 168, 277–284.

Fairén, A.G., Dohm, J.M., Baker, V.R., de Pablo, M.A., Ruiz, J., Ferris, J.C., Anderson, R.C., 2003. Episodic flood inundations of the northern plains of Mars. Icarus 165, 53–67.

Fairén, A.G., Fernández-Remolar, D., Dohm, J.M., Baker, V.R., Amils, R., 2004. Inhibition of carbonate synthesis in acidic oceans on early Mars. Nature 431, 423–426.

Fairén, A.G., Dohm, J.M., Uceda, E.R., Rodriguez, A.R., Baker, V.R., Fernández-Remolar, D., Schulze-Makuch, D., Amils, R., 2005. Prime candidate sites for astrobiological exploration through the hydrogeological history of Mars. Planet. Space Sci. 53, 1355–1375.

Feldman, W.C., Boynton, W.V., Tokar, R.L., Prettyman, T.H., Gasnault, O., Squyres, S.W., Elphic, R.C., Lawrence, D.J., Lawson, S.L., Maurice, S., McKinney, G.W., Moore, K.R., Reedy, R.C., 2002. Global distribution of neutrons from Mars: results from Mars Odyssey. Science 297, 75–78.

Ferrill, D.A., Wyrick, D.Y., Morris, A.P., Sims, D.W., Franklin, N.M., 2004. Dilational fault slip and pit chain formation on Mars. GSA Today 14, 4–12.

Ferris, J.C., Dohm, J.M., Baker, V.R., Maddock, T., 2002. Dark slope streaks on Mars: are aqueous processes involved? Geophys. Res. Lett. 29.

Fink, W., Dohm, J.M., Tarbell, M.A., Hare, T.M., Baker, V.R., 2005. Next-generation robotic planetary reconnaissance missions: a paradigm shift. Planet. Space Sci. 53, 1419–1426.

Formisano, V., Atreya, S., Encrenaz, T., Ignatiev, N., Giuranna, M., 2004. Detection of methane in the atmosphere of Mars. Science 306, 1758–1761.

Gendrin, A., Mangold, N., Bibring, J.P., Langevin, Y., Gondet, B., Poulet, F., Bonello, G., Quantin, C., Mustard, J., Arvidson, R., LeMouelic, S., 2005. Sulfates in martian layered terrains: the OMEGA/Mars express view. Science 307, 1587–1591.

Glamoclija, M., Garrel, L., Berthon, J., López-García, P., 2004. Biosignatures and bacterial diversity in hydrothermal deposits of Solfatara Crater, Italy. Geomicrobiol. J. 21, 529–541.

Golden, D.C., Ming, D.W., Morris, R.V., 2004. Acid-sulfate vapor reactions with basaltic tephra: an analog for martian surface processes. Lunar Planet. Sci. Conf. XXXV, 12 #1388 (abstract) (CD-ROM).

Golombek, M.P., 1989. Geometry of stresses around Tharsis on Mars. Lunar Planet. Sci. XX, 345–346 (abstract).

Golombek, M.P., Banerdt, W.B., Tanaka, K.L., Tralli, D.M., 1992. A prediction of Mars seismicity from surface faulting. Science 258, 979–981.

Golombek, M.P., Moore, H.J., Haldemann, A.F.C., Parker, T.J., Schofield, J.T., 1999. Assessment of Mars Pathfinder landing site predictions. J. Geophys. Res. 104, 8585–8594.

Gomes, R., Levison, H.F., Tsiganis, K., Morbidelli, A., 2005. Origin of the cataclysmic late heavy bombardment period of the terrestrial planets. Nature 435, 466–469.

Greeley, R., Guest, J.E., 1987. Geologic map of the eastern equatorial region of Mars. USGS Misc. Inv. Ser. Map I-1802B (1:15,000,000).

Grott, M., Kronberg, P., Hauber, E., Cailleau, B., 2007. Formation of the double rift system in the Thaumasia Highlands, Mars. J. Geophys. Res. 112, E06006.

Gulick, V.C., 1993. Magmatic intrusions and hydrothermal systems: Implications for the formation of small martian valleys. Ph.D. Thesis, University of Arizona, Tucson, Arizona.

Gulick, V.C., 1998. Magmatic intrusions and a hydrothermal origin for fluvial valleys on Mars. J. Geophys. Res. 103, 19,365–19,387.

Hartmann, W.K., Berman, D.C., 2000. Elysium Planitia lava flows: crater count chronology and geological implications. J. Geophys. Res. 105, 15011–15025.

Hartmann, W.K., Neukum, G., 2001. Cratering chronology and the evolution of Mars. Space Sci. Rev. 96, 165–194.

Hartmann, W.K., Malin, M.C., McEwen, A., Carr, M., Soderblom, L., Thomas, P., Danielson, E., James, P., Veverka, J., 1999. Recent volcanism on Mars from crater counts. Nature 397, 586–589.

Hauck II, S.A., Phillips, R.A., 2002. Thermal and crustal evolution of Mars. J. Geophys. Res. 107 (E7), 5052.

Head, J.W., Mustard, J.F., Kreslavsky, M.A., Milliken, R.E., Marchant, D.R., 2003a. Recent ice ages on Mars. Nature 426, 797–802.

Head, J.W., Wilson, L., Mitchell, K.L., 2003b. Generation of recent massive water floods at Cerberus Fossae, Mars by dike emplacement, cryospheric cracking, and aquifer groundwater release. Geophys. Res. Lett. 30 (11), 1577.

Head, J.W., Neukum, G., Jaumann, R., Hiesinger, H., Hauber, E., Carr, M., Masson, P., Foing, B., Hoffmann, H., Kreslavsky, M., Werner, S., Milkovich, S., van Gasselt, S., HRSC Co-Investigator Team, 2005. Tropical to mid-latitude snow and ice accumulation, flow and glaciation on Mars. Nature 434, 346–351.

Head, J.W., Marchant, D.R., Agnew, M.C., Fassett, C.I., Kreslavsky, M.A., 2006. Extensive valley glacier deposits in the northern mid-latitudes of Mars: evidence for Late Amazonian obliquity-driven climate change. Earth Planet. Sci. Lett. 241, 663–671.

Head III, J.W., Hiesinger, H., Ivanov, M.A., Kreslavsky, M.A., Pratt, S., Thompson, B.J., 1999. Possible ancient oceans on Mars: evidence from Mars Orbiter Laser Altimeter data. Science 286, 2134–2137.

Hurowitz, J.A., McLennan, S.M., Tosca, N.J., Arvidson, R.E., Michalski, J.R., Ming, D.W., Schröder, C., Squyres, S.W., 2006. In situ and experimental evidence for acidic weathering of rocks and soils on Mars. J. Geophys. Res. 111.

Irwin III, R.P., Maxwell, T.A., Howard, A.D., Craddock, R.A., Leverington, D.W., 2002. A large paleolake basin at the head of Ma'Adim Vallis, Mars. Science 296, 2209–2212.

Ivanov, B.A., 2001. Mars/Moon cratering rate ratio estimates. In: Kallenbach, R., Geiss, J., Hartmann, W.K. (Eds.), Chronology and Evolution of Mars. Kluwer Academic Publishers, Dordrecht, pp. 87–104.

Jackson, M.J., Pollack, H.N., 1984. On the sensitivity of parameterized convection to the rate of decay of internal heat sources. J. Geophys. Res. 89 (B12), 10103–10108.

Jaeger, W.L., Keszthelyi, L.P., McEwen, A.S., Dundas, C.M., Russell, P.S., 2007. Athabasca Valles, Mars: A lava-draped channel system. Science 317, 1709–1711.

Jakosky, B.M., Carr, M.H., 1985. Possible precipitation of ice at low latitudes of Mars during periods of high obliquity. Nature 315, 559–561.

Jöns, H.P., 1986. Arcuate ground undulations, gelifluxion-like features and "front tori" in the northern lowlands on Mars, what do they indicate? (abstract). Lunar Planet. Sci. Conf. XXVII, 404–405.

Kargel, J.S., Baker, V.R., Beget, J.E., Lockwood, J.F., Pewe, T.L., Shaw, J.S., Strom, R.G., 1995. Evidence of ancient continental glaciation in the martian northern plains. J. Geophys. Res. 100, 5351–5368.

Karunatillake, S.K., Squyres, S.W., Taylor, G.J., Keller, J., Gasnault, O., Evans, L.G., Reedy, R.C., Starr, R., Boynton, W., Janes, D.M., Kerry, K., Dohm, J.M., Sprague, A.L., Hamara, D., 2006. Composition of northern low-albedo regions of Mars: insights from the Mars Odyssey Gamma Ray Spectrometer. J. Geophys. Res. 111, E03S05.

Keller, J., Boynton, W.V., Baker, V.R., Dohm, J.M., Evans, L.G., Hamara, D., Janes, D., Karunatillake, S., Kerry, K., Reedy, R.C., Squyres, S.W., Starr, R.D., Taylor, J., the GRS Team, 2006. Equatorial and midlatitude distribution of chlorine measured by Mars Odyssey GRS. J. Geophys. Res. 111, E03S08.

Kiefer, W.S., 2003. Melting in the martian mantle: Shergottite formation and implications for present-day mantle convection on Mars. Meteor. Planet. Sci. 38 (12), 1815–1832.

Klingelhöfer, G., Morris, R.V., Bernhardt, B., Schröder, C., Rodionov, D.S., de Souza Jr., P.A., Yen, A., Gellert, R., Evlanov, E.N., Zubkov, B., Foh, J., Bonnes, U., Kankeleit, E., Gütlich, P., Ming, D.W., Renz, F., Wdowiak, T., Squyres, S.W., Arvidson, R.E., 2004. Jarosite and Hematite at Meridiani Planum from Opportunity's Mössbauer Spectrometer. Science 306, 1740–1745.

Komatsu, G., Dohm, J.M., Hare, T.M., 2004. Hydrogeologic processes of large-scale tectono-magmatic complexes in Mongolia-southern Siberia and on Mars. Geology 32, 325–328.

Krasnopolsky, V.A., 2006. Some problems related to the origin of methane on Mars. Icarus 180, 359–367.

Krasnopolshy, V.A., Maillard, J.P., Owen, T.C., 2004. Detection of methane in the marian atmosphere: evidence for life? Icarus 172, 537–547.

Kring, D.A., Cohen, B.A., 2002. Cataclysmic bombardment throughout the inner solar system. J. Geophys. Res. 107 (E2), 4-1–4-6.

Kuzmin, R.O., Greeley, R., Landheim, R., Cabrol, N.A., Framer, J.D., 2004. Geologic map of the MTM-15182 and MTM-15187 quadrangles, Gusev Crater-Ma'adim Vallis region, Mars. US Geol. Survey Map I-2666.

Langevin, Y., Poulet, F., Bibring, J.-P., Gondet, B., 2005. Sulfates in the North Polar region of Mars detected by OMEGA/Mars Express. Science 307, 1584–1586.

Laskar, J., Robutel, P., 1993. The chaotic obliquity of the planets. Nature 361, 608–612.

Laskar, J., Correia, A.C.M., Gastineau, M., Joutel, F., Levard, B., Robutel, P., 2004. Long term evolution and chaotic diffusion of the insolation quantities of Mars. Icarus 170, 343–364.

Li, Z.X., Li, X.H., Kinny, P.D., Wang, J., Zhang, S., Zhou, H., 2003. Geochronology of Neoproterozoic syn-rift magmatism in the Yangtze Craton, South China and correlations with other continents: evidence for a mantle superplume that broke up Rodinia. Precambrian Research 122, 85–109.

Lucchitta, B.K., Ferguson, H.M., Summers, C., 1986. Sedimentary deposits in the northern lowland plains, Mars. J. Geophys. Res. 91, E166–E174.

Lucchitta, B.K., McEwen, A.S., Clow, G.D., Geissler, P.E., Singer, R.B., Schultz, R.A., Squyres, S.W., 1992. The canyon system on Mars. In: Mars. University of Arizona Press, Tucson, pp. 453–492.

Malin, M.C., 1979. Mars: evidence of indurated deposits of fine materials. NASA Conf. Pub. 2072, 54.

Malin, M.C., Edgett, K.S., 2000. Sedimentary rocks on early Mars. Science 290, 1927–1937.

Márquez, A., Fernández, C., Anguita, F., Farelo, A., Anguita, J., de la Casa, M.-A., 2004. New evidence for a volcanically, tectonically, and climatically active Mars. Icarus 172, 573–581.

Maruyama, S., 1994. Plume tectonics. J. Geol. Soc. Japan 100, 24–49.

McEwen, A.S., Preblich, B.S., Turtle, E.P., Artemieva, N.A., Golombek, M.P., Hurst, M., Kirk, R.L., Burr, D.M., Christensen, P.R., 2005. The rayed crater Zunil and interpretations of small impact craters on Mars. Icarus 176, 351–381.

McEwen, A.S., and 14 others, 2007. Mars Reconnaissance Orbiter's High Resolution Imaging Science Experiment (HiRISE). J. Geophys. Res. 112, doi:10.1029/2005JE002605.

McGill, G.E., 1985. Age and origin of large martian polygons (abstract). Lunar. Planet. Sci. Conf. XVI, 534–535.

McGovern, P.J., Solomon, S.C., Smith, D.E., Zuber, M.T., Simons, M., Wieczorek, M.A., Phillips, R.J., Neumann, G.A., Aharonson, O., Head, J.W., 2002. Localized gravity/topography admittance and correlation spectra on Mars: implications for regional and global evolution. J. Geophys. Res. 107 (E12), 5136.

McLennan, S.M., 2001. Crustal heat production and the thermal evolution of Mars. Geophys. Res. Lett. 28, 4019–4022.

McSween, H.Y., 1994. What we have learned from Mars from SNC meteorites. Meteoritics 29, 757–779.

McSween, H.Y., Treiman, A.H., 1998. Martian meteorites. In: Papike, J.J. (Ed.), Planetary Materials. Rev. Mineral. 36, pp. 6-1–6-46.

McSween Jr., H.Y., 2002. The rocks of Mars, from far and near. Meteor. Planet. Sci. 37, 7–25.

Mège, D., Ernst, R.E., 2001. Contractional effects of mantle plumes on Earth, Mars, and Venus. In: Ernst, R.E., Buchan, K.L. (Eds.), Mantle plumes: their identification through time. Geol. Soc. Am. Spec. Pap. 352, 103–140.

Melosh, H.J., 1988. The rocky road to panspermia. Nature 332, 687–688.

Milkovich, S.M., Head, J.W., Marchant, D.R., 2006. Debris-covered piedmont glaciers along the northwest flank of the Olympus Mons scarp: evidence for low-latitude ice accumulation during the Late Amazonian of Mars. Icarus 181, 388–407.

Mischna, M.A., Richardson, M.I., Wilson, R.J., McCleese, D.J., 2003. On the orbital forcing of martian water and CO_2 cycles: a general circulation model study with simplified volatile schemes. J. Geophys. Res. 108.

Mitchell, K.L., Wilson, L., 2003. Mars: a geologically active planet. Astron. Geophys. 44, 4.16–4.20.

Miyamoto, H., Dohm, J.M., Beyer, R.A., Baker, V.R., 2004. Fluid dynamical implications of anastomosing slope streaks on Mars. J. Geophys. Res. 109.

Moore, H.J., 2001. Geologic map of the Tempe-Mareotis region of Mars. US Geol. Survey Map I-2727.

Morris, E.C., Tanaka, K.L., 1994. Geologic map of the Olympus Mons region of Mars. USGS Misc. Inv. Ser. Map I-2327.

Morris, E.C., Masursky, H., Applebee, D.J., Strobell, M.E., 1991. Geologic map of science study area 3, Olympus Rupes, Mars (special MTM 15132 quadrangle). USGS Misc. Inv. Ser. Map I-2001.

Mouginis-Mark, P.J., 1985. Volcano/ground ice interactions in Elysium Planitia, Mars. Icarus 64, 265–284.

Mouginis-Mark, P.J., 1990. Recent water release in the Tharsis region of Mars. Icarus 84, 362–373.

Mumma, M.J., Novak, R.E., DiSanti, M.A., Bonev, B.P., Dello Russo, N., 2004. Detection and mapping of methane and water on Mars. Bull. Am. Astron. Soc. 36, 11274.

Murchie, S., 49 others, 2007. Compact Reconnaissance Imaging Spectrometer for Mars (CRISM) on Mars Reconnaissance Orbiter (MRO). J. Geophys. Res. 112, doi:10.1029/2006JE002682.

Nakamura, Y., 1980. Shallow moonquakes: are they comparable to earthquakes? Lunar Planet. Sci. Conf. 11, 789–790.

Nelson, D.M., Greeley, R., 1999. Geology of Xanthe Terra outflow channels and the Mars Pathfinder landing site. J. Geophys. Res. 104, 8653–8669.

Neukum, G., Ivanov, B.A., Hartmann, W.K., 2001. Cratering records in the inner solar system in relation to the lunar reference system. In: Kallenbach, R., Geiss, J., Hartmann, W.K. (Eds.), Chronology and Evolution of Mars. Kluwer Academic Publishers, Dordrecht, pp. 55–86.

Neukum, G., Jaumann, R., Hoffmann, H., Hauber, E., Head, J.W., Basilevsky, A.T., Ivanov, B.A., Werner, S.C., van Gasselt, S., Murray, J.B., McCord, T., 2004. The HRSC Co-Investigator Team, Recent and episodic volcanic and glacial activity on Mars revealed by the High Resolution Stereo Camera. Nature 432, 971–979.

Nimmo, F., Stevenson, D.J., 2001. Estimates of martian crustal thickness from viscous relaxation of topography. J. Geophys. Res. 106, 5085–5098.

Nimmo, F., Tanaka, K., 2005. Early crustal evolution of Mars. Ann. Rev. Earth Planet. Sci., 133–161.

Nyquist, L.E., Bogard, D.D., Shih, C.Y., Greshake, A., Stöffler, D., Eugster, O., 2001. Ages and geologic histories of martian meteorites. In: Kallenbach, R., Geiss, J., Hartmann, W.K. (Eds.), Chronology and Evolution of Mars. Kluwer Academic Publishers, Dordrecht, pp. 105–164.

Onstott, T.C., McGown, D., Kessler, J., Sherwood Lollar, B., Lehmann, K.K., Clifford, S.M., 2006. Martian CH4: sources, flux, and detection. Astrobiology 6, 377–395.

Orsi, G., De Vita, S., Di Vito, M., 1996. The restless, resurgent Campi Flegrei nested caldera (Italy): constrains on its evolution and configuration. J. Vulcanol. Geotherm. Res. 74, 179–214.

Parker, T.J., Schneeberger, D.M., Pieri, D.C., Saunders, R.S., 1987. Geomorphic evidence for ancient seas on Mars. In: Symposium on Mars: Evolution of its Climate and Atmosphere. LPI Technical Report 87-01, pp. 96–98.

Parker, T.J., Gorsline, D.S., Saunders, R.S., Pieri, D.C., Schneeberger, D.M., 1993. Coastal geomorphology of the martian northern plains. J. Geophys. Res. 98, 11061–11078.

Pieri, D.C., 1976. Distribution of small channels on the martian surface. Icarus 27, 25–50.

Plescia, J.B., Saunders, R.S., 1982. Tectonic history of the Tharsis region, Mars. J. Geophys. Res. 87, 9775–9791.

Plescia, J.B., 2003. Cerberus Fossae, Elysium, Mars: a source for lava and water. Icarus 164, 79–95.

Plescia, J.B., Roth, L.E., Saunders, R.S., 1980. Tectonic features of southeast Tharsis. In: Reports of Planetary Geology Program, NASA Tech. Memo. 81776, pp. 68–70.

Pollack, J.B., Kasting, J.F., Richardson, S.M., Poliakoff, K., 1987. The case for a wet, warm climate on early Mars. Icarus 71, 203–224.

Poulet, F., Bibring, J.-P., Mustard, J.F., Gendrin, A., Mangold, N., Langevin, Y., Arvidson, R.E., Gondet, B., Gomez, C., the OMEGA Team, 2005. Phyllosilicates on Mars and implications for the Early Mars History. Nature 481, 623–627.

Prieto-Ballesteros, O., Kargel, J.S., Fairén, A.G., Fernández-Remolar, D., Dohm, J.M., Amils, R., 2006. Interglacial clathrate destabilization on Mars: possible contributing source of its atmospheric methane. Geology 4, 49–152.

Rice Jr., J.R., DeHon, R.A., 1996. Geologic map of the Darvel Quadrangle (MTM 20052), Maja Valles region of Mars. USGS Misc. Inv. Ser. Map I-2432 (1:500,000).

Richardson, M.I., Mischna, M.A., 2005. Long-term evolution of transient liquid water on Mars. J. Geophys. Res. 110, E03003.

Rieder, R., Gellert, R., Anderson, R.C., Brückner, J., Clark, B.C., Dreibus, G., Economou, T., Klingelhöfer, G., Lugmair, G.W., Ming, D.W., Squyres, S.W., d'Uston, C., Wänke, H., Yen, A., Zipfel, J., 2004. Chemistry of rocks and soils at Meridiani Planum from the Alpha Particle X-ray Spectrometer. Science 306, 1746–1749.

Rifkin, M.K., Mustard, J.F., 2001. Global distribution of unique surface processes imaged by the Mars Orbital Camera. Lunar Planet. Sci. Conf. (CD-ROM) XXXII abstract 1698.

Robinson, M.S., Mouginis-Mark, P.J., Zimbelman, J.R., Wu, S.S.C., Ablin, K.K., Howington-Kraus, A.E., 1993. Chronology, eruption duration, and atmospheric contribution of the martian volcano, Apollinaris patera. Icarus 104, 301–323.

Rosi, M., Sbrana, A., 1987. The Phlegraean Fields, CNR. Quad. Ric. Sci. 114, 175.

Rotto, S.L., Tanaka, K.L., 1995. Geologic/geomorphologic map of the Chryse Planitia region of Mars. USGS Misc. Inv. Ser. Map I-2441 (1:5,000,000).

Russell, P.S., Head, J.W., 2003. Elysiim-Utopia flows as mega-lahars: a model of dike intrusion, cryosphere cracking, and water-sediment release. J. Geophys. Res. 108.

Schorghofer, N., Aharonson, O., Khatiwala, S., 2002. Slope streaks on Mars: correlations with surface properties and the potential role of water. Geophys. Res. Lett. 29.

Schott, B., van den Berg, A.P., Yuen, D.A., 2001. Focused time-dependent martian volcanism from chemical differentiation coupled with variable thermal conductivity. Geophys. Res. Lett. 28, 4271–4274.

Schubert, G., Solomon, S.C., Turcotte, D.L., Drake, M.J., Sleep, H.N., 1992. Origin and thermal evolution of Mars. In: Kieffer, H.H., et al. (Eds.), Mars. The University of Arizona Press, pp. 147–183.

Schultz, P.H., Lutz, A.B., 1988. Polar wandering on Mars. Icarus 73, 91–141.

Schultz, R.A., Tanaka, K.L., 1994. Lithospheric buckling and thrust structures on Mars: the Coprates rise and south Tharsis ridge belt. J. Geophys. Res. 99, 8371–8385.

Schulze-Makuch, D., Irwin, L.N., 2002. Energy cycling and hypothetical organisms in Europa's ocean. Astrobiology 2, 105–121.

Schulze-Makuch, D., Irwin, L.N., 2004. Life in the Universe: Expectations and Constraints. Springer, Berlin, New York.

Schulze-Makuch, D., Dohm, J.M., Fairén, A.G., Baker, V.R., Fink, W., Strom, R.G., 2005a. Venus, Mars, and the ices on Mercury and the Moon: astrobiological implications and proposed mission designs. Astrobiology 5, 778–795.

Schulze-Makuch, D., Irwin, L.N., Lipps, J.H., LeMone, D., Dohm, J.M., Fairén, A.G., 2005b. Scenarios for the evolution of life on Mars. J. Geophys. Res. 110, E12S23.

Schulze-Makuch, D., Dohm, J.M., Fan, C., Fairén, A.G., Rodriguez, J.A.P., Baker, V.R., Fink, W., 2007. Exploration of hydrothermal targets on Mars. Icarus 189, 308–324.

Scott, D.H., 1993. Geologic map of the MTM 25057 and 25052 quadrangles, Kasei Valles region of Mars. USGS Misc. Inv. Ser. I-Map 2208 (1:500,000).

Scott, D.H., Chapman, M.G., 1991. Geologic map of science study area 6, Memnonia region of Mars (MTM-10172). USGS Misc. Inv. Ser. Map I-2084 (1:500,000).

Scott, D.H., Dohm, J.M., 1990a. Faults and ridges: Historical development in Tempe Terra and Ulysses Patera regions of Mars. In: Proceedings of the 20th Lunar and Planetary Science Conference, Part 2: Lunar and Planetary Institute, Houston, March 13–17, 1989, pp. 503–513.

Scott, D.H., Dohm, J.M., 1990b. Chronology and global distribution of fault and ridge systems on Mars. In: Proceedings of the 20th Lunar and Planetary Science Conference, Part 2: Lunar and Planetary Institute, Houston, March 13–17, 1989, pp. 487–501.

Scott, D.H., Dohm, J.M., 1997. Mars Structural Geology and Tectonics: Encyclopedia of Planetary Sciences. Van Nostrand Reinhold, New York, pp. 461–463.

Scott, D.H., Tanaka, K.L., 1982. Ignimbrites of the Amazonis Planitia region of Mars. J. Geophys. Res. 87, 1179–1190.

Scott, D.H., Tanaka, K.L., 1986. Geologic map of the western equatorial region of Mars. USGS Misc. Inv. Ser. Map I-1802-A (1:15,000,000).

Scott, D.H., Zimbelman, J.R., 1995. Geologic map of Arsia Mons volcano, Mars, USGS Misc. Inv. Ser. Map I-2480 (1:1,000,000).

Scott, D.H., Dohm, J.M., Applebee, D.J., 1993. Geologic map of science study area 8, Apollinaris Patera region of Mars. USGS Misc. Inv. Ser. Map I-2351 (1:500,000).

Scott, D.H., Dohm, J.M., Rice Jr., J.W., 1995. Map of Mars showing channels and possible paleolake basins. USGS Misc. Inv. Ser. Map I-2461 (1:30,000,000).

Scott, D.H., Dohm, J.M., Zimbelman, J.R., 1998. Geologic map of Pavonis Mons volcano, Mars. USGS Misc. Inv. Ser. Map I-2561 (1:1,000,000).

Segura, T.L., Toon, O.B., Colaprete, A., Zahnle, K., 2002. Environmental effects of large impacts on Mars. Science 298, 1977–1980.

Shean, D.E., Head, J.W., Marchant, D.R., 2005. Origin and evolution of a cold-based tropical mountain glacier on Mars: the Pavonis Mons fan-shaped deposit. J. Geophys. Res. 110.

Sleep, N.H., 1994. Martian plate tectonics. J. Geophys. Res. 99, 5,639–5,655.

Sleep, N.H., 2000. Evolution of the mode of convection within terrestrial planets. J. Geophys. Res. 105, 17,563–17,578.

Smith, M.D., Bandfield, J.L., Christensen, P.R., Richardson, M.L., 2003. Thermal Emission Imaging system (THEMIS) infrared observations of atmospheric dust and water ice cloud optical depth. J. Geophys. Res. 108, 5515.

Solomon, S.C., Head, J.W., 1982. Evolution of the Tharsis province of Mars: the importance of heterogeneous lithospheric thickness and volcanic construct. J. Geophys. Res. 87, 9755–9774.

Solomon, S.C., Anderson, D.L., Banerdt, W.B., Butler, R.G., Davis, P.M., Dunnebier, F.K., Nakamura, Y., Okal, E.A., Phillips, R.J., 1991. Scientific rationale and requirements for a global seismic network on Mars. Tech. Rep. No. 91-02, Lunar and Planetary Institute, Houston, TX.

Solomon, S.C., Aharonson, O., Aurnou, J.M., Banerdt, W.B., Carr, M.H., Dombard, A.J., Frey, H.V., Golombek, M.P., Hauck II, S.A., Head III, J.W., Jakosky, B.M., Johnson, C.L., McGovern, P.J., Neumann, G.A., Phillips, R.J., Smith, D.E., Zuber, M.T., 2005. New perspectives on ancient Mars. Science 307, 1214–1220.

Spohn, T., 1991. Mantle differentiation and thermal evolution of Mars, Mercury, and Venus. Icarus 90, 222–236.

Squyres, S.W., Grotzinger, J.P., Arvidson, R.E., Bell III, J.F., Calvin, W., Christensen, P.R., Clark, B.C., Crisp, J.A., Farrand, W.H., Herkenhoff, K.E., Johnson, J.R., Klingelhöfer, G., Knoll, A.H., McLennan, S.M., McSween Jr., H.Y., Morris, R.V., Rice Jr., J.W., Rieder, R., Soderblom, L.A., 2004. In situ evidence for an ancient aqueous environment at Meridiani Planum, Mars. Science 306, 1709.

Stevenson, D.J., 2001. Mars' core and magnetism. Nature 412, 214–219.

Strom, R.G., Malhotra, R., Ito, T., Yoshida, F., Kring, D.A., 2005. The origin of planetary impactors in the inner solar system. Science 309, 1847–1850.

Sullivan, R., Thomas, P., Veverka, J., Malin, M., Edgett, K.S., 2001. Mass movement slope streaks imaged by the Mars Orbiter Camera. J. Geophys. Res. 106, 23,607–23,633.

Swindle, T.D., Treiman, A.H., Lindstrom, D.J., Burkland, M.K., Cohen, B.A., Grier, J.A., Li, B., Olson, E.K., 2000. Noble gases in iddingsite from the Lafayette meteorite: evidence for liquid water on Mars in the last few hundred million years. Meteor. Planet. Sci. 35, 107–115.

Tanaka, K.L., 1986. The stratigraphy of Mars. Proceedings of the 17th Lunar Planetary Science Conference, Part 1, J. Geophys. Res 91, E139–E158.

Tanaka, K.L., Davis, P.A., 1988. Tectonic history of the Syria Planum province of Mars. J. Geophys. Res. 93, 14,893–14,917.

Tanaka, K.L., Golombek, M.P., Banerdt, W.B., 1991. Reconciliation of stress and structural histories of the Tharsis region of Mars. J. Geophys. Res. 96, 15,617–15,633.

Tanaka, K.L., Chapman, M., Scott, D.H., 1992. Geologic map of the Elysium region of Mars. USGS Misc. Inv. Ser. Map I-2147 (1:5,000,000).

Tanaka, K.L., Dohm, J.M., Lias, J.H., Hare, T.M., 1998. Erosional valleys in the Thaumasia region of Mars: hydrothermal and seismic origins. J. Geophys. Res. 103, 31,407–31,419.

Tanaka, K.L., Skinner, J.A., Hare, T.M., Joyal, T., Wenker, A., 2003. Resurfacing history of the northern plains of Mars based on geologic mapping of Mars Global Surveyor data. J. Geophys. Res. 108, 12.

Tanaka, K.L., Skinner Jr., J.A., Hare, T.M., 2005. Geologic map of the northern plains of Mars. USGS Misc. Inv. Ser. Map SIM-2888, scale 1:15,000,000.

Taylor, G.J., Boynton, W., Brückner, J., Wänke, H., Dreibus, G., Kerry, K., Keller, J., Reedy, R., Evans, L., Starr, R., Squyres, S., Karunatillake, S., Gasnault, O., Maurice, S., d'Uston, C., Englert, P., Dohm, J.M., Baker, V., Hamara, D., Janes, D., Sprague, A., Kim, K., Drake, D., 2006. Bulk composition and early differentiation of Mars. J. Geophys. Res. 111, E03S10.

Tosca, N.J., McLennan, S.M., Lindsley, D.H., Schoonen, M.A.A., 2004. Acid-sulfate weathering of synthetic martian basalt: the acid fog model revisited. J. Geophys. Res. 109 (E05003).

Touma, J., Wisdom, J., 1993. The chaotic obliquity of Mars. Science 259, 1294–1296.

Valentino, G.M., Cortecci, G., Franco, E., Stanzione, D., 1999. Chemical and isotopic compositions of minerals and waters from Campi Flegrei volcanic system, Naples, Italy. J. Volc. Geoth. Res. 91, 329–344.

Wang, A., Bell III, J., Li, R., Johnson, J.R., Farrand, W., Arvidson, R.E., Crumpler, L., Squyres, S.W., Herkenhoff, K., Knudson, A., Chen, W., Athena team, 2007. Sulfate-rich soils exposed by Spirit rover at multiple locations in Gusev Crater on Mars. In: Seventh International Conference on Mars, #3348 (abstract).

Wänke, H., Dreibus, G., 1994. Chemistry and accretion history of Mars. Philos. Trans. R. Soc. London A 349, 285–293.

Wänke, H., Brückner, J., Dreibus, G., Rieder, R., Ryabchikov, I., 2001. Chemical composition of rocks and soils at the Pathfinder site. Space Sci. Rev. 96, 317–330.

Watson, E.B., Harrison, T.M., 2005. Zircon thermometer reveals minimum melting conditions on earliest Earth. Science 308, 841–844.

Wieczorek, M.A., Zuber, M.T., 2004. The thickness of the martian crust: improved constraits from geoid-to-topography ratios. J. Geophys. Res. 109, E01009.

Wise, D.U., Golombek, M.P., McGill, G.E., 1979. Tharsis province of Mars: geologic sequence, geometry, and a deformation mechanism. Icarus 38, 456–472.

Wohletz, K., Orsi, G., de Vita, S., 1995. Eruptive mechanisms of the Neapolitan Yellow Tuff interpreted from stratigraphic, chemical and granulometric data. J. Volcanol. Geotherm. Res. 67, 263–290.

Wyrick, D., Ferrill, D.A., Morris, A.P., Colton, S.L., Sims, D.W., 2004. Distribution, morphology, and origins of martian pit crater chains. J. Geophys. Res. 109, E06005.

Zimbelman, J.R., Craddock, R.A., Greeley, R., 1994. Geologic map of the MTM -15147 quadrangle, Mangala Valles region of Mars. USGS Misc. Inv. Ser. Map I-2402 (1:500,000).

Zuber, M.T., 2001. The crust and mantle of Mars. Nature 412, 220–227.

Zuber, M.T., Solomon, S.C., Phillips, R.J., Smith, D.E., Tyler, G.L., Aharonson, O., Balmino, G., Banerdt, W.B., Head, J.W., Johnson, C.L., Lemoine, F.G., McGovern, P.J., Neumann, G.A., Rowlands, D.D., Zhong, S., 2000. Internal structure and early thermal evolution of Mars from Mars Global Surveyor topography and gravity. Science 287, 1788–1793.